

Impacts of aviation fuel sulfur content on climate and human health

Zarashpe Z Kapadia^{1,2}, Dominick V. Spracklen², Steve R. Arnold², Duncan J. Borman³, Graham W. Mann^{2,4}, Kirsty J. Pringle², Sarah A. Monks^{2,*,**}, Carly L. Reddington², François Benduhn⁵, Alexandru Rap², Catherine E. Scott², Edward W. Butt², Masaru Yoshioka²

¹Doctoral Training Centre in Low Carbon Technologies, Energy Research Institute, School of Process Environmental and Materials Engineering, University of Leeds, Leeds, UK

²Institute for Climate and Atmospheric Science, School of Earth and Environment, University of Leeds, Leeds, UK

³Centre for Computational Fluid Dynamics, School of Civil Engineering, University of Leeds, Leeds, UK

⁴National Centre for Atmospheric Science, School of Earth and Environment, University of Leeds, Leeds, UK

⁵Institute for Advanced Sustainability Studies, Potsdam, Germany

*now at: Cooperative Institute for Research in Environmental Sciences, University of Colorado Boulder, Boulder, Colorado, USA

**now at: Chemical Sciences Division, NOAA Earth System Research Laboratory, Boulder, Colorado, USA

Abstract

Aviation emissions impact both air quality and climate. Using a coupled tropospheric chemistry-aerosol microphysics model we investigate the effects of varying aviation fuel sulfur content (FSC) on premature mortality from long-term exposure to aviation-sourced PM_{2.5} (particulate matter with a dry diameter of <2.5 μm) and on the global radiation budget due to changes in aerosol and tropospheric ozone. We estimate that present-day non-CO₂ aviation emissions with a typical FSC of 600 ppm result in ~3,600 [95% CI: 1,310–5,890] annual premature mortalities globally due to increases in cases of cardiopulmonary disease and lung cancer, resulting from increased surface PM_{2.5} concentrations. We quantify the global annual mean combined radiative effect (RE_{comb}) of non-CO₂ aviation emissions as –13.3 mW m⁻²; from increases in aerosols (direct radiative effect and cloud albedo effect) and tropospheric ozone.

Ultra-low sulfur jet fuel (ULSJ; FSC = 15 ppm) has been proposed as an option to reduce the adverse health impacts of aviation-induced PM_{2.5}. We calculate that swapping the global aviation fleet to ULSJ fuel would reduce the global aviation-induced mortality rate by ~620 [95% CI: 230–1020] mortalities a⁻¹ and increase RE_{comb} by +7.0 mW m⁻².

We explore the impact of varying aviation FSC between 0–6000 ppm. Increasing FSC increases aviation-induced mortality, while enhancing climate cooling through increasing the aerosol cloud albedo effect (CAE). We explore the relationship between the injection altitude of aviation emissions and the resulting climate and air quality impacts. Compared to the standard aviation emissions distribution, releasing aviation emissions at the ground increases global aviation-induced mortality and produces a net warming effect, primarily through a reduced CAE. Aviation emissions injected at the surface are 5 times less effective at forming cloud condensation nuclei, reducing the aviation-induced CAE by a factor of 10. Applying high FSCs at aviation cruise altitudes combined with ULSJ fuel at lower altitudes results in reduced aviation-induced mortality and increased negative RE compared to the baseline aviation scenario.

53 1 Introduction

54 Aviation is the fastest growing form of transport (Eyring et al., 2010; Lee et al., 2010; Uherek et al., 2010), with
55 a projected growth in passenger air traffic of 5% yr⁻¹ until 2030 (Barrett et al., 2012; ICAO, 2013), and a
56 projected near doubling of emissions by 2025, relative to 2005 (Eyers et al., 2004). These emissions, and
57 changes to them, have both climate and air quality impacts (Lee et al., 2009; Barrett et al., 2010; Woody et al.,
58 2011; Barrett et al., 2012).

59
60 Aviation emits a range of gas-phase and aerosol pollutants that can influence climate. Emissions of carbon
61 dioxide (CO₂) from aviation warm the climate (Lee et al., 2009; Lee et al., 2010). Emissions of nitrogen oxides
62 (NO_x) warm the climate through tropospheric ozone (O₃) formation, which acts as a greenhouse gas, and cool
63 climate via a decrease in the lifetime of the well-mixed greenhouse gas methane (CH₄) through increases in
64 the OH radical (Holmes et al., 2011; Myhre et al., 2011). Sulfate and nitrate aerosols, formed from aviation
65 sulfur dioxide (SO₂) and NO_x emissions and through altered atmospheric oxidants, lead to a cooling (Unger,
66 2011; Righi et al., 2013; Dessens et al., 2014), and black carbon (BC) emissions result in a warming (Balkanski
67 et al., 2010). Additionally, the formation of persistent linear contrails and contrail-cirrus from aircraft leads to
68 warming (Lee et al., 2010; Rap et al., 2010; Burkhardt and Karcher, 2011). Overall, aviation emissions are
69 thought to have a warming impact on climate, with net radiative forcing (RF) estimated as +55 mW m⁻²
70 (excluding cirrus cloud enhancement) (Lee et al., 2010).

71
72 Previous studies have separately assessed the impacts of aviation through different atmospheric species.
73 Short-term O₃ has been estimated to have a radiative effect ranging between 6–36.5 mW m⁻² (Sausen et al.,
74 2005; Köhler et al., 2008; Hoor et al., 2009; Lee et al., 2009; Holmes et al., 2011; Myhre et al., 2011; Unger,
75 2011; Frömming et al., 2012; Skowron et al., 2013; Unger et al., 2013; Khodayari et al., 2014; Brasseur et al.,
76 2015). The aerosol direct effect is highly uncertain [–28 to +20 mW m⁻²] (Righi et al., 2013), with the direct
77 aerosol effects for sulfate ranging between –0.9 to –7 mW m⁻² (Sausen et al., 2005; Fuglestedt et al., 2008;
78 Lee et al., 2009; Balkanski et al., 2010; Unger, 2011; Gettelman and Chen, 2013; Brasseur et al., 2015), nitrate
79 ranging between –4 to –7 mW m⁻² (Unger et al., 2013; Brasseur et al., 2015), BC ranging between 0.1–0.3 mW
80 m⁻² (Sausen et al., 2005; Fuglestedt et al., 2008; Lee et al., 2009; Balkanski et al., 2010; Unger, 2011;
81 Gettelman and Chen, 2013; Unger et al., 2013; Brasseur et al., 2015), and for organic carbon (OC) ranging
82 between –0.67 to –0.01 mW m⁻² (Sausen et al., 2005; Fuglestedt et al., 2008; Lee et al., 2009; Balkanski et al.,
83 2010; Unger, 2011; Gettelman and Chen, 2013; Unger et al., 2013). Few studies estimate the aerosol cloud
84 albedo effect (aCAE) from aviation: Righi et al. (2013) assessed the aCAE to be –15.4±10.6 mW m⁻² while
85 Gettelman and Chen (2013) estimate –21±11 mW m⁻².

86
87 Aviation emissions can increase atmospheric concentrations of fine particulate matter with a dry diameter of
88 <2.5 µm (PM_{2.5}). Short-term exposure to PM_{2.5} can exacerbate existing respiratory and cardiovascular ailments,
89 while long-term exposure can result in chronic respiratory and cardiovascular diseases, lung cancer, chronic
90 changes in physiological functions and mortality (Pope et al., 2002; World Health Organisation, 2003; Ostro,
91 2004). In the U.S. aviation emissions are estimated to lead to adverse health effects in ~11,000 people (ranging
92 from mortality, respiratory ailments and hospital admissions due to exacerbated respiratory conditions) and
93 ~23,000 work loss days per annum (Ratliff et al., 2009). Landing and take-off aviation emissions increase PM_{2.5}
94 concentrations, particularly around airports (Woody et al., 2011), increasing US mortality rates by ~160 per
95 annum.

96
97 Previous studies have estimated the number of premature mortalities due to exposure to pollution resulting
98 from aviation emissions. Barrett et al. (2012) and Barrett et al. (2010) used the methodology of Ostro (2004)
99 to estimate that aviation emissions are responsible for ~10,000 premature mortalities a⁻¹ due increases in
100 cases of cardiopulmonary disease and lung cancer. Yim et al. (2015) using the same methodology but with the
101 inclusion of the Rapid Dispersion Code (RDC) to simulate the local air quality impacts of aircraft ground level
102 emissions estimated 13,920 (95% CI: 7,220–20,880) mortalities a⁻¹. Morita et al. (2014) using the integrated
103 exposure–response (IER) model from Burnett et al. (2014) to derive relative risk (RR) estimate that aviation
104 results in 405 (95% CI: 182–648) mortalities a⁻¹ due to increases in cases of lung cancer, stroke, ischemic heart
105 disease, trachea, bronchus, and chronic obstructive pulmonary disease. Jacobson et al. (2013) estimate 310

106 (95% CI: -400 to 4,300) mortalities a⁻¹ from aviation emissions due to cardiovascular effects. Taking these
107 studies in account, the different methodologies applied and modes of mortality investigated aviation is
108 estimated to be responsible for between 310–13,920 mortalities a⁻¹.

109
110 The introduction of cleaner fuels and pollution control technologies can improve ambient air quality and
111 reduce adverse health effects of fossil fuel combustion (World Health Organisation, 2005). One proposed
112 solution to reduce the adverse health effects of aviation-induced PM_{2.5} is the use of ultra-low sulfur jet fuel
113 (ULSJ), reducing the formation of sulfate aerosol (Barrett et al., 2012; Barrett et al., 2010; Ratliff et al., 2009;
114 Hileman and Stratton, 2014). ULSJ fuels typically have a fuel sulfur content (FSC) of 15 ppm, compared with an
115 FSC of between 550–750 ppm in standard aviation fuels (Barrett et al., 2012). The current global regulatory
116 standard for aviation fuel is a maximum FSC of 3000 ppm (Ministry of Defence, 2011; ASTM International,
117 2012).

118
119 Despite the potential for decreased emission of SO₂, application of ULSJ fuel will not completely remove the
120 impacts of aviation on PM_{2.5}. It is estimated that over a half of aviation-attributable surface-level sulfate is
121 associated with oxidation of non-aviation SO₂ by OH produced from aviation NO_x emissions, and not directly
122 produced from aviation-emitted SO₂ (Barrett et al., 2010). Therefore, even a completely desulfurised global
123 aviation fleet would likely contribute a net source of sulfate PM_{2.5}. Nevertheless, previous work has shown
124 that the use of ULSJ fuel reduces global aviation-induced PM_{2.5} by ~23%, annually avoiding ~2300 (95% CI:
125 890–4200) mortalities (Barrett et al., 2012).

126
127 Altering the sulfur content of aviation fuel also modifies the net climate impact of aviation emissions. A
128 reduction in fuel sulfur content reduces the formation of cooling sulfate aerosols (Unger, 2011; Barrett et al.,
129 2012), increasing the net warming effect of aviation emissions. The roles of sulfate both in climate cooling and
130 in increasing surface PM_{2.5} concentrations mean that policy makers must consider both health and climate
131 when considering effects from potential reductions in sulfur emissions from a given emissions sector (Fiore et
132 al., 2012).

133
134 In this study, we investigate the impacts of changes in the sulfur content of aviation fuel on climate and human
135 health. A coupled tropospheric chemistry-aerosol microphysics model is used to quantify global atmospheric
136 responses in aerosol and O₃ to varying FSC scenarios. Radiative effects due to changes in tropospheric O₃ and
137 aerosols are calculated using a radiative transfer model the impacts of changes in surface PM_{2.5} on human
138 health are estimated using concentration response functions. Using a coupled tropospheric chemistry-aerosol
139 microphysics model that includes nitrate aerosol allows us to assess the impacts of nitrate and aerosol indirect
140 effects in addition to the ozone and aerosol direct effects that have been more routinely calculated.

141

142 **2 Methods**

143

144 **2.1 Coupled chemistry-aerosol microphysics model**

145 **2.1.1 Model description**

146 We use GLOMAP-mode (Mann et al., 2010), embedded within the 3-D off-line Eulerian chemical transport
147 model TOMCAT (Arnold et al., 2005; Chipperfield, 2006). Meteorology (wind, temperature and humidity) and
148 large scale transport is specified from interpolation of 6-hourly European Centre for Medium Range Weather
149 Forecasts (ECMWF) reanalysis (ERA-40) fields (Chipperfield, 2006; Mann et al., 2010). Cloud fraction and cloud
150 top pressure fields are taken from the International Satellite Cloud Climatology Project (ISCCP-D2) archive for
151 the year 2000 (Rossow and Schiffer, 1999).

152

153 GLOMAP-mode is a two-moment aerosol microphysics scheme representing particles as an external mixture
154 of 7 size modes (4 soluble and 3 insoluble) (Mann et al., 2010). We use the nitrate-extended version of
155 GLOMAP-mode (Benduhn et al., 2016) which, as well as tracking size-resolved sulfate, BC, OC, sea-salt and
156 dust components, also includes a dissolution solver to accurately characterise the size-resolved partitioning of

157 ammonia and nitric acid into ammonium and nitrate components in each soluble mode. Aerosol components
158 are assumed to be internally mixed within each mode. GLOMAP-mode includes representations of nucleation,
159 particle growth via coagulation, condensation and cloud processing, wet and dry deposition, and in- and
160 below-cloud scavenging (Mann et al., 2010).

161
162 TOMCAT includes a tropospheric gas-phase chemistry scheme (inclusive of O_x - NO_y - HO_x), treating the
163 degradation of C_1 - C_3 non-methane hydrocarbons (NMHCs) and isoprene, together with a sulfur chemistry
164 scheme (Spracklen et al., 2005; Breider et al., 2010; Mann et al., 2010). The tropospheric chemistry is coupled
165 to aerosol as described in Breider et al. (2010).

166
167 The nitrate-extended version of the TOMCAT-GLOMAP-mode coupled model used in this investigation
168 employs a hybrid solver to simulate the dissolution of semi-volatile inorganic gases (such as H_2O , HNO_3 , HCl
169 and NH_3) into the aerosol-liquid-phase.

170
171 Emissions of DMS are calculated using monthly mean sea-water concentrations of DMS from (Kettle and
172 Andreae, 2000), driven by ECMWF winds and sea-air exchange parameterisations from Nightingale et al.
173 (2000). Emissions of SO_2 are included from both continuous (Andres and Kasgnoc, 1998) and explosive
174 volcanoes (Halmer et al., 2002), and wildfires for year 2000 (Van Der Werf et al., 2003; Dentener et al., 2006).
175 Anthropogenic SO_2 emissions (including industrial, power-plant, road-transport, off-road-transport and
176 shipping sectors) are representative of the year 2000 (Cofala et al., 2005). Emissions of monoterpenes and
177 isoprene are from Guenther et al. (1995). NH_3 emissions are from the EDGAR inventory (Bouwman et al., 1997).
178 NO_x emissions are considered from anthropogenic (Lamarque et al., 2010), natural (Lamarque et al., 2005)
179 and biomass burning (van der Werf et al., 2010) sources.

180
181 Annual mean emissions of BC and OC aerosol from fossil fuel and biofuel combustion are from Bond et al.
182 (2004). Monthly wildfire emissions are taken from the GFED v1 (Global Fire Emissions Database) for the year
183 2000 (Van Der Werf et al., 2003). For primary aerosol emissions we use geometric mean diameters (D_g) with
184 standard deviations as described by Mann et al. (2010).

185
186 Here, we ran simulations at a horizontal resolution of $2.8^\circ \times 2.8^\circ$ with 31 hybrid σ -p levels extending from the
187 surface to 10 hPa. All simulations were conducted for 16 months from September 1999 to December 2000
188 inclusive, with the first four months discarded as spin-up time.

189

190 **2.1.2 Model evaluation**

191 GLOMAP has been extensively evaluated against observations including comparisons of speciated aerosol
192 mass (Mann et al., 2010; Spracklen et al., 2011b), aerosol number (Mann et al., 2010; Spracklen et al., 2010)
193 and cloud condensation nuclei (CCN) concentrations (Spracklen et al., 2011a). TOMCAT simulated fields have
194 been evaluated against observations, with CO and O_3 evaluated against aircraft observations (Arnold et al.,
195 2005), Mediterranean summertime ozone against satellite observations (Richards et al., 2013), along with O_3
196 evaluated against satellite observations (Chipperfield et al., 2015). Benduhn et al. (2016) shows that simulated
197 surface concentrations of NO_3 and NH_4 are in reasonable agreement with observations in Europe, the U.S. and
198 East Asia. Here we focus our evaluation on the aerosol vertical profile and as well as nitrate aerosol which has
199 not been evaluated previously.

200

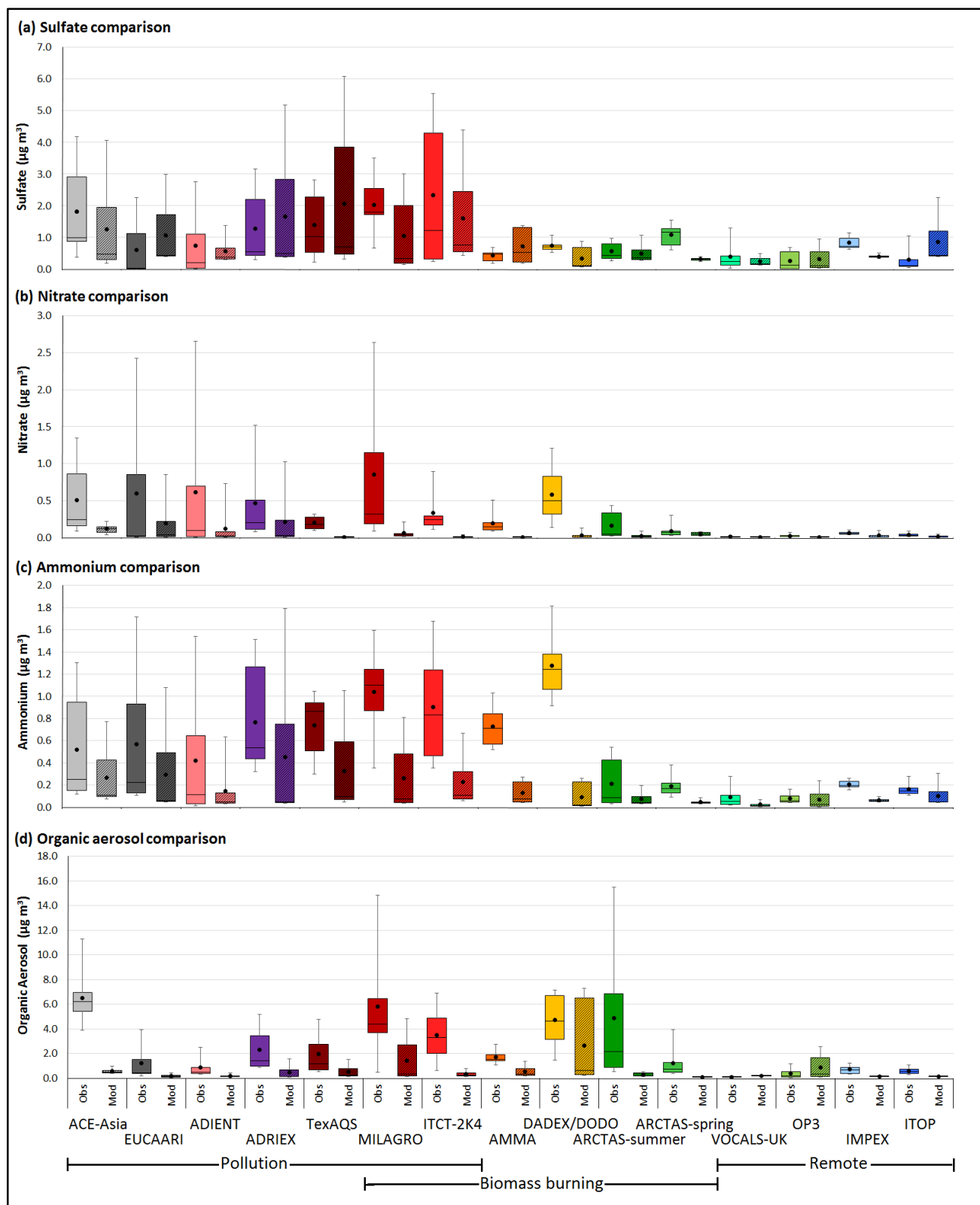
201 Fig. 1 presents simulated sulfate, nitrate, ammonium and organic aerosol mass concentrations in comparison
202 to airborne observations compiled by Heald et al. (2011). The supplementary information presents the flight
203 paths of each of the aircraft field campaigns used in the study compiled by Heald et al. (2011) (Figure S1), and
204 details of each of the aircraft field campaigns used (Table S1). Observations were predominantly made using
205 an Aerodyne Aerosol Mass Spectrometer (AMS). Simulated profiles are for year 2000, while observational
206 aerosol profiles are from field campaigns conducted between 2001 and 2008.

207

208

209

210 **Fig. 1: Comparison of observed (Obs) and simulated (Mod) (a) sulfate; (b) nitrate; (c) ammonium, and; (d)**
 211 **organic aerosol mass concentrations. Observations are from airborne field campaigns compiled by Heald et**
 212 **al. (2011). Mean values are represented by black dots, median values as shown by horizontal lines, while**
 213 **boxes denote the 25th and 75th percentiles, and whiskers denote the 5th and 95th percentile values.**



214 Overall we find the model overestimates sulfates [NMB = +16.9%], while underestimating nitrates [NMB = -
 215 60.7%], ammonium [NMB = -47.1%] and organic aerosols (OA) [NMB = -56.2%]. Model skill varies dependant
 216 on the conditions affecting each field campaign. To explore this, we use the broad stratification of the field
 217 campaigns into anthropogenic pollution, biomass burning and remote conditions as used by Heald et al. (2011)

218 and shown in Fig. 1. The model underestimates aerosol concentrations in biomass burning regions [sulfate
219 NMB = -14.9%; nitrate NMB = -79.4%; ammonium NMB = -68.7%, and; OA NMB = -74.5%]. The model
220 performs better in polluted [sulfate NMB = +31.6%; nitrate NMB = -56.2%; ammonium NMB = -28.6%, and;
221 OA NMB = -40.9%], and remote regions [sulfate NMB = +25.4%; nitrate NMB = -6.4%; ammonium NMB = -
222 20.2%, and; OA NMB = -41.5%].

223

224 The overestimation of sulfate aerosol is likely due to the decline in anthropogenic SO₂ emissions in Europe and
225 the US between 2000–2008 (Vestreng et al., 2007; Hand et al., 2012). An underestimation of OA has been
226 reported previously (Heald et al., 2011; Spracklen et al., 2011b) and is likely due to an underestimate in SOA
227 formation in the model. Whitburn et al. (2015) found biomass burning emissions of NH₃ may be
228 underestimated which would affect a number of our comparisons.

229

230 The model underestimation of organic and inorganic aerosol components in biomass burning influenced
231 regions could partly be due to very concentrated plumes in these regions affecting campaign mean
232 concentrations. There is a large uncertainty in biomass burning emissions and some evidence that they may
233 be underestimated (Kaiser et al., 2012), which may contribute to the model bias. Biomass burning emissions
234 also have large interannual variability (van der Werf et al., 2010; Wiedinmyer et al., 2011), meaning that using
235 year specific emissions might improve comparison against observations in these regions. Underestimation in
236 Arctic inorganic aerosol, which will affect the ARCTAS comparisons, is a well-known problem in models,
237 likely related to problems with model wet deposition and emissions (Shindell et al., 2008; Eckhardt et al.,
238 2015). The model underestimate over West Africa (AMMA, DADEX and DODO campaigns) is likely due to
239 a combination of errors in biomass burning emissions and poorly constrained emission sources from
240 anthropogenic activity (Knippertz et al., 2015).

241

242 Fig. 2 presents simulated ozone concentration profiles in comparison to ozonesonde observations compiled
243 by Tilmes et al. (2012). Observations were compiled from three networks, comprising of 41 stations with
244 continuous sampling from 1995 to 2011: (i) The World Ozone and Ultraviolet Data Center (WOUDC)
245 (<http://www.woudc.org/>); (ii) the Global Monitoring Division (GMD, [ftp:// ftp.cmdl.noaa.gov/ozwv/ozone/](ftp://ftp.cmdl.noaa.gov/ozwv/ozone/)),
246 and (iii) The Southern Hemisphere ADDitional OZonesondes (SHADOZ) (Tilmes et al., 2012).

247

248 Regional model-observation comparison profiles presented in Fig. 2 demonstrate good agreement between
249 the model and ozonesonde profiles, while demonstrating regional variations driven by variations in
250 tropopause height, showing no evidence of systematic model bias in the upper troposphere. Notable
251 differences are seen between simulated and observed ozone profiles over the Praha launch site in Western
252 Europe, with the model greatly overestimating observed ozone.

253

254 Evaluation of ozone model bias is conducted for the troposphere, using a chemical tropopause definition of
255 150 ppbv ozone, as previously used by Stevenson et al. (2013), Young et al. (2013) and Rap et al. (2015). We
256 find the model overestimates global ozone concentrations [NMB = +7.0%] with overestimates in Western
257 Europe [+18.9%] and the Northern Hemisphere Polar West [NMB = +14.4%] regions and underestimates over
258 the Atlantic/Africa [NMB = -11.0%] and Southern Hemisphere Polar [NMB = -4.6%] regions.

259

260 Differences between model and observational profiles can in part be explained by the differences in years of
261 simulation and observation, a poor representation of deep convection resulting in model underestimations in
262 the tropics and overestimations downwind (Thompson et al., 1997), in tandem with reductions in
263 anthropogenic NO_x emissions over this time period (Konovalov et al., 2008).

264

265

266

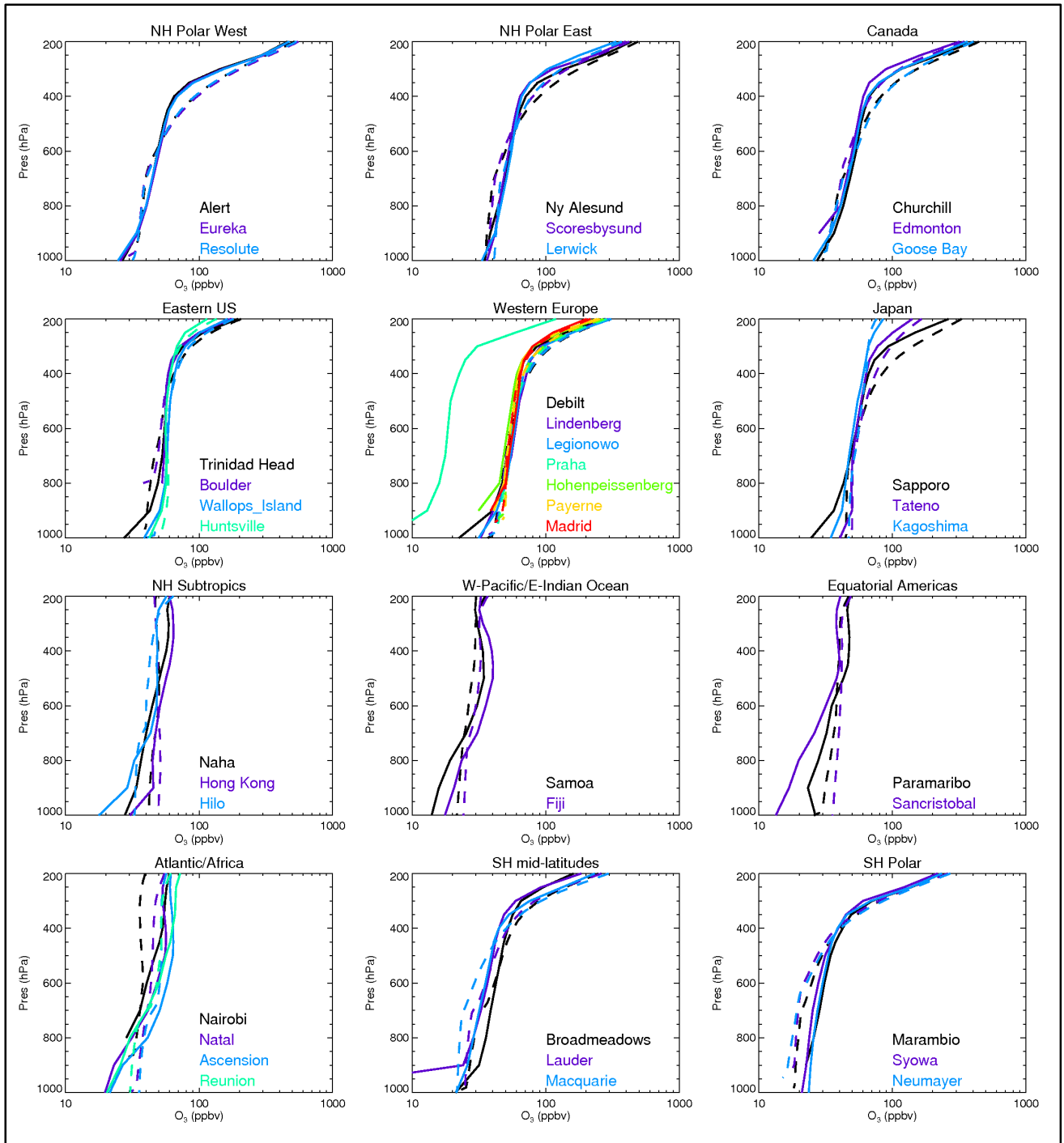
267

268

269

270
271
272

Fig. 2: Comparison of observed (solid lines) and simulated (dashed lines) ozone profiles. Observations are taken from ozonesonde observations, and arranged by launch location regions according to Tilmes et al. (2012).



273
274
275
276
277
278
279
280
281
282

283 2.2 Aviation emissions

284 Aircraft emit NO_x, carbon monoxide (CO), SO₂, BC, OC and hydrocarbons (HCs). The historical emissions dataset
 285 for the CMIP5 (5th Coupled Model Intercomparison Project) model simulations used by the IPCC 5th Assessment
 286 Report only included NO_x and BC aviation emissions (Lamarque et al., 2009). Recently there have been efforts
 287 to add HCs, CO and SO₂ emissions to aviation emission inventories (Eyers et al., 2004; Quantify Integrated
 288 Project, 2005-2012; Wilkerson et al., 2010).

289
 290 Here we develop a new 3-D civil aviation emissions dataset for the year 2000, based on CMIP5 historical
 291 aviation emissions (Lamarque et al., 2009). The new dataset includes emissions of NO_x, CO, SO₂, BC, OC, and
 292 HCs. In contrast to existing datasets which provide a general emissions index for HCs (Eyers et al., 2004) we
 293 speciate HCs as formaldehyde (HCHO), ethane (C₂H₆), propane (C₃H₈), methanol (CH₃OH), acetaldehyde
 294 (CH₃CHO), and acetone ((CH₃)₂CO).

295
 296 Table 1 describes our new emissions dataset. NO_x and BC emissions are taken directly from Lamarque et al.
 297 (2009). We calculate fuelburn from BC emissions data and the BC emissions index (Eyers et al., 2004) as used
 298 by Lamarque et al. (2009). Following DuBois and Paynter (2006), we assume that BC emissions scale linearly
 299 with fuel consumption. We estimate emissions for other species using our calculated aviation fuelburn in
 300 combination with published species-specific emissions indices (EI reported in g kg⁻¹ of fuel). Emission indices
 301 for CO and SO₂ are from the FAA's aviation environmental design tool (AEDT) (Wilkerson et al., 2010). OC
 302 emissions are calculated using a BC:OC ratio of 4 (Hopke, 1985; Bond et al., 2004); resulting in an EI within the
 303 range determined by Wayson et al. (2009). Speciated hydrocarbon emissions are calculated from experimental
 304 data following the methodology of Wilkerson et al. (2010) using experimental data from Knighton et al. (2007)
 305 and Anderson et al. (2006), in conjunction with operating parameters suggested by the Airbus Flight Crew
 306 Training manual (Airbus, 2008).

307
 308 **Table 1: Aviation emissions indices and total annual emissions for year 2000**
 309

Species	Emissions index (g kg ⁻¹ of fuel)	Global emissions for year 2000 (Tg of species)	Range of annual global emissions from previous studies (Tg of species)
NO _x	13.89 ^a	2.786	1.98–3.286 ^{a,b,j,h,i,k,l}
CO	3.61 ^b	0.724	0.507–0.679 ^{b,h,i,j}
HCHO	1.24 ^{c,d}	0.249	0.01205 ^b
C ₂ H ₆	0.0394 ^e	0.007899	0.00051 ^b
C ₃ H ₈	0.03 ^e	0.006014	0.00444 ^b
CH ₃ OH	0.22 ^d	0.044	0.00177 ^b
CH ₃ CHO	0.33 ^d	0.066	0.00418 ^b
(CH ₃) ₂ CO	0.18 ^d	0.036	0.00036 ^b
SO ₂	1.1760 ^b	0.236	0.182–0.221 ^{a,b,h,i,j}
BC	0.0250 ^a	0.005012	0.0039–0.0068 ^{a,b,h,i,j,k}
OC	0.00625 ^{f,g}	0.001253	0.003 ^{b,i}

^a(Eyers et al., 2004), ^b(Wilkerson et al., 2010), ^c(Spicer et al., 1994), ^d(Knighton et al., 2007),
^e(Anderson et al., 2006), ^f(Bond et al., 2004), ^g(Hopke, 1985), ^h(Olsen et al., 2013), ⁱ(Unger, 2011),
^j(Lee et al., 2010), ^k(Lamarque et al., 2010), ^l(Quantify Integrated Project, 2005-2012)

310
 311 Our global aviation emissions typically lie within the range of previous studies (Table 1). Our SO₂ emissions are
 312 greater than those used by Wilkerson et al. (2010) for 2006, despite the use of the same EI. This is due to the
 313 greater global fuelburn considered by the base inventory used to develop our emissions inventory (Eyers et
 314 al., 2004; Lamarque et al., 2010). Our estimated OC emissions are lower than the emissions estimated in the
 315 AEDT 2006 inventory, due to the lower EI applied here. The lower EI_{OC} applied here (in comparison to
 316 Wilkerson et al. (2010)) is a due to the phase of flight considered when deriving the AEDT emissions inventory;
 317 where they derive EI_{OC} focusing on airport operations at ground level condition acknowledging the risk of

318 overestimating aviation OC emissions, while in comparison we consider aircraft operations after ground idle
 319 conditions which risks underestimating aviation OC emissions.

320

321 We calculate the geometric mean diameter (D_g) for internally mixed BC/OC particles as 50.5 nm from the mean
 322 particle mass derived using the particle number emissions index (Eyers et al., 2004) and a constant standard
 323 deviation set to $\sigma = 1.59$ nm.

324

325 2.3 Fuel sulfur content simulations

326 To explore the impact of aviation FSC on climate and air quality we performed a series of 11 global model
 327 experiments (Table 2). In 7 of these model experiments FSC values were varied globally between zero and
 328 6000 ppm. Three further simulations varied the vertical distribution of aviation emissions. The first simulation
 329 collapses all aviation emissions to ground level (GROUND), in order to compare an equivalent ground emission
 330 source and its effects. Two simulations (SWITCH1 and SWITCH2), use a low FSC (15 ppm) applied below the
 331 cruise phase of flight (<8.54 km altitude) (Lee et al., 2009; Köhler et al., 2013) combined with a high FSC at
 332 altitudes above. The SWITCH1 scenario increases FSC in line with our HIGH scenario above 8.54 km, while in
 333 the SWITCH2 scenario, emissions are scaled such that total global sulfur emissions are the same as the
 334 standard simulation (NORM), resulting in a FSC of 1420 ppm above 8.54 km. Results from all simulations are
 335 compared against a simulation with aviation emissions excluded (NOAVI).

336

337 **Table 2: FSC and global SO₂ emissions applied in each model experiment.**

Scenario name	Description	FSC (ppm)	Total SO ₂ emitted (Tg)
NOAVI	No aviation emissions	n/a	0.0
NORM	Standard aviation emissions scenario	600	0.236
DESUL	Desulfurised case	0	0.0
ULSJ	Ultra low sulfur jet fuel	15	0.006
HALF	Half FSC of normal case	300	0.118
TWICE	Twice FSC of normal case	1200	0.472
HIGH	FSC at international specification limit	3000	1.179
OVER	Twice FSC specification limit	6000	2.358
GROUND	All emissions emitted at surface level (FSC as NORM)	600	0.236
SWITCH1	ULSJ FSC to 8.54 km, HIGH FSC content above	15/3000	0.491
SWITCH2	ULSJ FSC to 8.54 km, FSC = 1420 ppm above	15/1420	0.236

338

339 2.4 Radiative impacts

340 We calculate the aerosol direct radiative effect (aDRE), aerosol cloud albedo effect (aCAE) and tropospheric
 341 O₃ direct radiative effect (O3DRE) using the offline Edwards and Slingo (1996) radiative transfer model. The
 342 radiative transfer model considers 6 bands in the shortwave (SW) and 9 bands in the longwave (LW), adopting
 343 a delta-Eddington 2 stream scattering solver at all wavelengths. The top-of-the-atmosphere (TOA) aerosol
 344 aDRE and aCAE are calculated using the methodology described in Rap et al. (2013) and Spracklen et al.
 345 (2011a), with the method for O3DRE as in Richards et al. (2013). To determine the aCAE we calculated cloud
 346 droplet number concentrations (CDNCs) using the monthly mean aerosol size distribution simulated by
 347 GLOMAP combined with parameterisations from Nenes and Seinfeld (2003), updated by Fountoukis and
 348 Nenes (2005) and Barahona et al. (2010). CDNC were calculated with a prescribed updraft velocity of 0.15 m
 349 s⁻¹ over ocean and 0.3 m s⁻¹ over land. Changes to CDNC were then used to perturb the effective radii of cloud
 350 droplets in low- and mid-level clouds (up to 600 hPa). The aDRE, aCAE and O3DREs for each aviation emissions
 351 scenario are calculated as the difference in TOA net (SW + LW) radiative flux compared to the NOAVI
 352 simulation.

353

354 2.5 Health effects

355 We calculate excess premature mortality from cardiopulmonary diseases and increases in cases of lung cancer
356 due to long-term exposure to aviation-induced PM_{2.5} (Ostro, 2004). Using this function allows us to compare
357 directly with previous studies (Barrett et al., 2012; Yim et al., 2015); in future work estimates are required with
358 updated methodologies (Burnett et al., 2014). PM_{2.5} is used as a measure of likely health impacts because
359 chronic exposure is associated with adverse human health impacts including morbidity and mortality (Dockery
360 et al., 1993; Pope and Dockery, 2006).

361
362 We relate annual excess mortality to annual mean surface PM_{2.5} via a concentration response-function (CRF)
363 (Ostro, 2004). This response-function considers concentrations of PM_{2.5} for a perturbed case (X) (defined by
364 aviation emissions scenarios from Table 2) in relation to a baseline case with no aviation emissions (X₀)
365 (NOAVI). To calculate excess mortality, the relative risk (RR) for both cardiopulmonary disease and lung cancer
366 are calculated according to Ostro (2004) using a function of baseline (X₀) and perturbed (X) PM_{2.5}
367 concentrations, and the disease specific cause-specific coefficient (β):
368

$$370 \text{ RR} = \left[\frac{(X+1)}{(X_0+1)} \right]^\beta \quad (1)$$

369
371
372 β coefficients for cardiopulmonary disease mortality of 0.15515 [95% CI = 0.05624–0.2541] and lung cancer of
373 0.232 [95% CI = 0.086–0.379] are used (Pope et al., 2002; Ostro, 2004). The 95% confidence interval (CI) in β
374 allow low-, mid- and high-range mortality values to be calculated. The attribution factor (AF) from the
375 exposure to air pollution is calculated using equation (2):
376

$$377 \text{ AF} = (\text{RR} - 1) / \text{RR} \quad (2)$$

378
379 Excess mortality (E) for both cardiopulmonary disease and lung cancer are calculated using baseline mortality
380 rates (B), the fraction of the population over 30 years old (P₃₀), along with the AF:
381

$$382 \text{ E} = \text{AF} \times \text{B} \times \text{P}_{30} \quad (3)$$

383
384 Global population data is taken from the Gridded World Population (GWP; version3) project (Center for
385 International Earth Science Information Network, 2012) with country specific data on the fraction of the
386 population under 30.
387

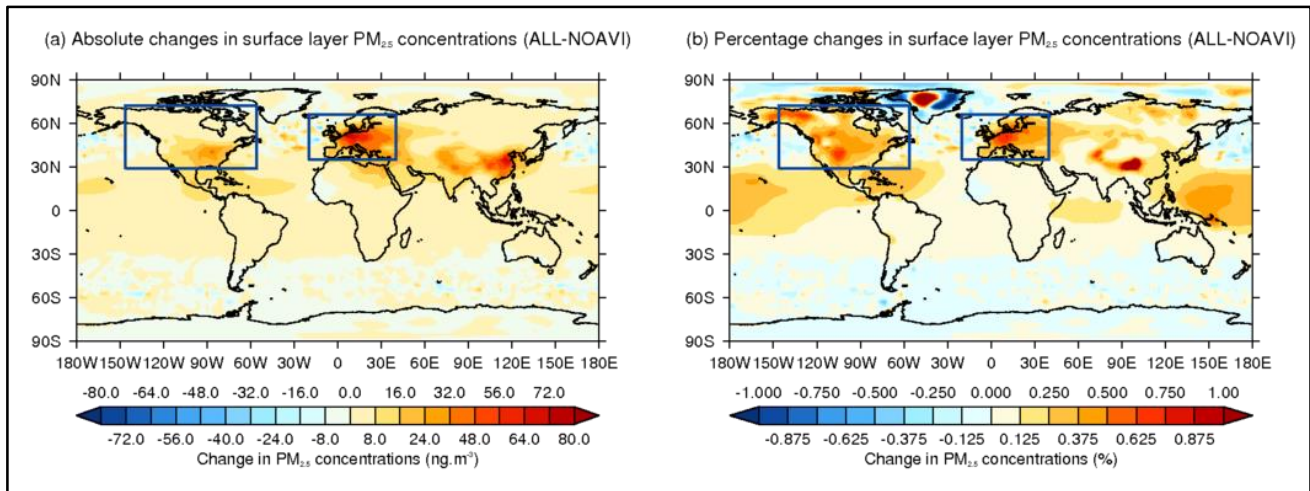
388 3 Results

389

390 3.1 Surface PM_{2.5}

391 Fig. 3 shows the simulated impact of aviation emissions with standard FSC (FSC = 600 ppm; NORM) on surface
392 PM_{2.5} concentrations. Aviation increases annual mean PM_{2.5} concentrations by up to ~80 ng m⁻³ (relative to
393 the NOAVI simulation) over Central Europe and Eastern China (Fig. 3(a)). Aviation emissions result in largest
394 fractional changes in annual mean PM_{2.5} concentrations (up to 0.8%) over North America and Europe (Fig.
395 3(b)).
396
397
398
399
400
401
402

403 **Fig. 3: Impact of aviation emissions (FSC = 600 ppm) on surface annual mean PM_{2.5} concentrations. (a)**
 404 **absolute (NORM–NOAVI) and (b) percentage changes. Boxes show the European (20°–40°E, 35°N–66°N) and**
 405 **North American (146°W–56°W, 29°N–72°N) regions.**



406 Fig. 4 shows the impact of aviation emissions on global and regional mean PM_{2.5} concentrations, as a function
 407 of FSC. With standard FSC (FSC = 600 ppm), aviation increases global mean surface PM_{2.5} concentrations by
 408 3.9 ng m⁻³; with increases in PM_{2.5} dominated by sulfates [56.2%], nitrates [26.0%] and ammonium [16.0%].
 409 Aviation emissions increase European annual mean PM_{2.5} concentrations by 20.3 ng m⁻³ (Fig. 4(b)),
 410 substantially more than over North America (Fig. 4(c)) where an annual mean increase of 6.3 ng m⁻³ is
 411 simulated. Increased PM_{2.5} is dominated by nitrates, both over Europe [55.5%] and over North America
 412 [44.4%]. Sulfates contribute up to 44.6% of increases in PM_{2.5} over North America, and 30.0% over Europe.
 413

414 The use of ULSJ fuel (FSC = 15 ppm) reduces global annual mean surface aviation-induced PM_{2.5} concentrations
 415 (in relation to the NORM case) by 35.7% [1.4 ng m⁻³] (Fig. 4); predominantly due to changes in sulfate [-1.4 ng
 416 m⁻³; -62.1%] and ammonium [-0.2 ng m⁻³; -37.9%], which are marginally offset by very small increases in
 417 nitrates [+3.2x10⁻³ ng m⁻³; +0.3%]. Aviation emissions also leads to small changes to other aerosol components
 418 of +0.2 ng; which includes natural aerosols such as dust [+0.3 ng m⁻³; +61.8%], sodium [-19.5%] and chloride
 419 from sea-salt [-19.5%] with the changes due to changes in aerosol lifetimes, along with changes in BC [-7.9%]
 420 and OC [-19.3%].
 421

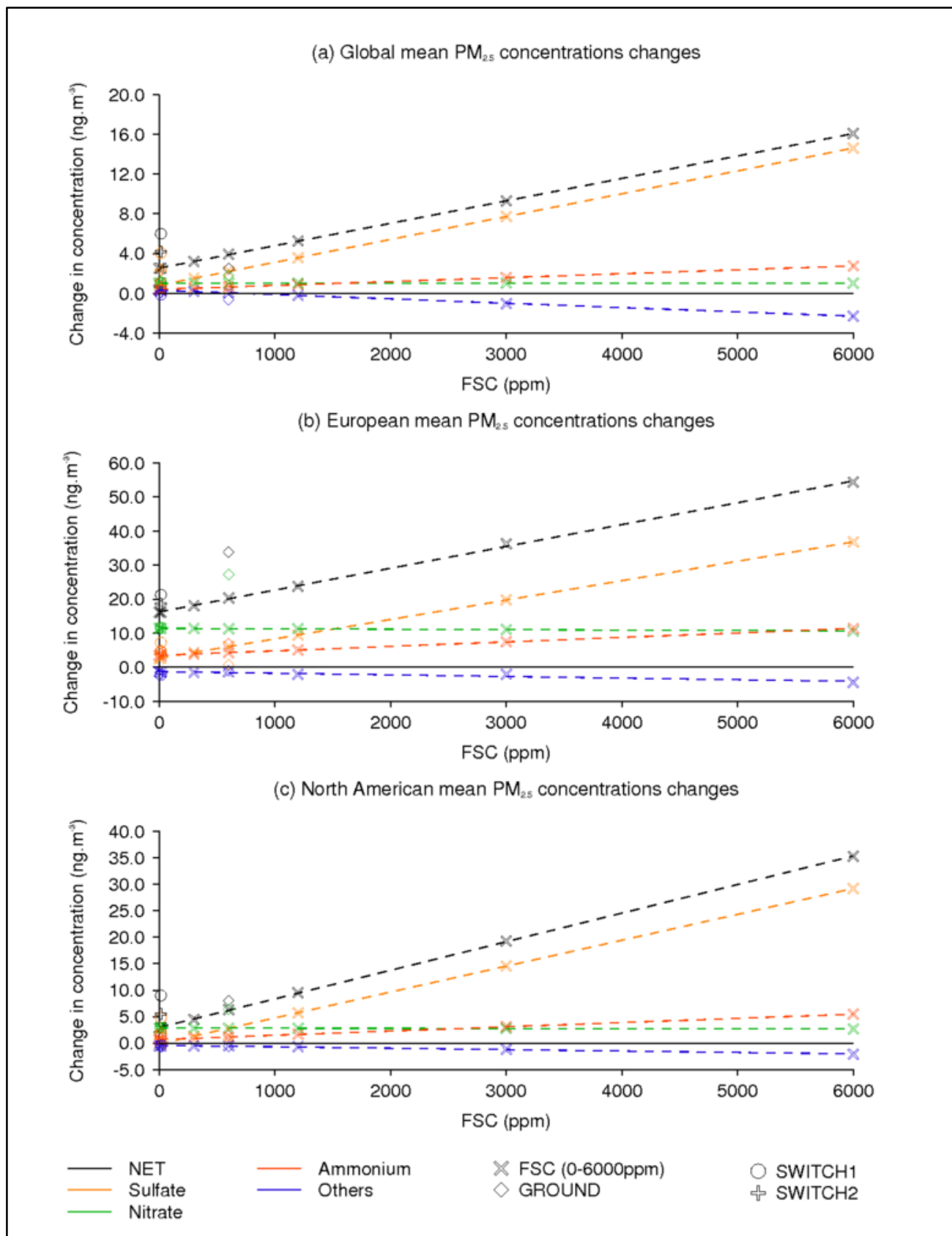
422 In comparison to the global mean, switching to the use of ULSJ fuel in aviation larger absolute reductions in
 423 PM_{2.5} of -4.2 ng m⁻³ are simulated over Europe [Δ sulfate = -3.4 ng m⁻³; Δ nitrate = +0.1 ng m⁻³; Δ ammonium =
 424 -0.8 ng m⁻³; and Δ others = -0.1 ng m⁻³] and of -3.4 ng m⁻³ over North America [Δ sulfate = -2.9 ng m⁻³; Δ nitrate
 425 = +0.02 ng m⁻³; Δ ammonium = -0.5 ng m⁻³; and Δ others = -0.01 ng m⁻³] (Fig. 4 (b,c)). Over North America,
 426 swapping to ULSJ fuel reduces aviation-induced PM_{2.5} by 53.4%, while a smaller reduction of 20.5% is simulated
 427 over Europe. The smaller fractional change in PM_{2.5} over Europe is caused by smaller reductions in aviation-
 428 induced sulfate [-55.9%] and ammonium [-18.4%] compared to over North America, which sees a reduction
 429 in ammonium of 41.6% and a reduction in sulfates of 103% indicating that over the US the ULSJ fuel scenario
 430 sees a reduction in sulfates in relation to a NOAVI scenario.
 431

432 Complete desulfurisation of jet fuel (FSC = 0 ppm; DESUL) reduces global mean aviation-induced surface PM_{2.5}
 433 concentrations by 36.5% [-1.43 ng m⁻³], with changes in sulfates [-1.40 ng m⁻³; -63.5%] and ammonium [-0.24
 434 ng m⁻³; -38.8%] dominating. Under this scenario the reductions in surface sulfate PM_{2.5} from aviation are 57.3%
 435 over Europe and 105% over North America. ULSJ fuel therefore gives similar results to complete
 436 desulfurisation, due to the very small sulfur emission from ULSJ fuel (Table 2).
 437

438 In summary, increases in FSC result in increased surface PM_{2.5}, due to increased sulfate outweighing the small
 439 reductions in nitrate. Simulated changes in sulfate, nitrate, ammonium and total PM_{2.5} are linear ($R^2 > 0.99$, p -
 440 value < 0.001 globally and for all individual regions) with respect to FSC (Fig. 4). Larger emission perturbations
 441 would likely lead to a non-linear response in atmospheric aerosol. The impact of variations in FSC on PM_{2.5} are

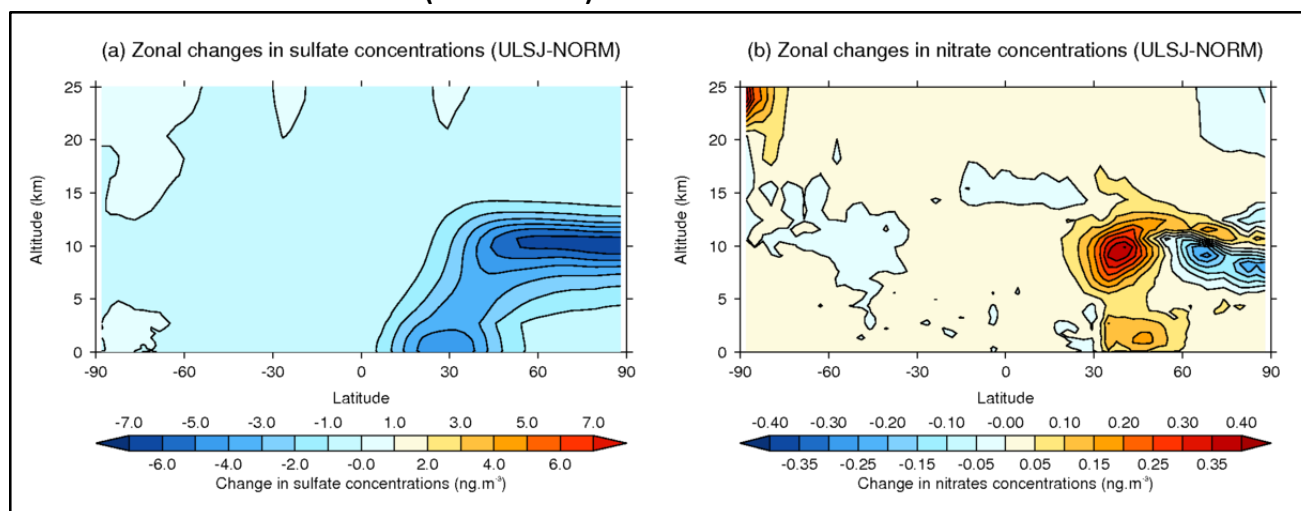
442 regionally variable; over Europe changes in PM_{2.5} concentrations are observed to be more sensitive to changes
 443 in FSC than over North America, and the global domain.

444
 445 **Fig. 4: Impact of aviation FSC on (a) global, (b) European (20°–40°E, 35°N–66°N), (c) North American (146°W–**
 446 **56°W, 29°N–72°N) surface annual mean PM_{2.5} mass concentrations: FSC variations (×), GROUND (◇),**
 447 **SWITCH1 (–), and SWITCH2 (+) simulations. Solid lines demonstrate the linear relationship between FSC**
 448 **and PM_{2.5}.**



449

450 **Fig. 5: Simulated differences in zonal annual mean sulfate (a) and nitrate (b) concentrations from the use of**
 451 **ULSJ fuel relative to standard fuel (ULSJ–NORM).**



452

453 Fig. 5 shows the impact of changing to ULSJ fuel on zonal mean sulfate and nitrate concentrations relative to
 454 standard fuel (NORM). Table 3 reports the global aerosol burden from aviation under different emission
 455 scenarios. With standard FSC (FSC = 600 ppm), the global aviation-induced aerosol burden is 16.9 Gg,
 456 dominated by sulfates (76.3%) and nitrates (33.4%). The use of ULSJ (FSC = 15 ppm) reduces the global aerosol
 457 burden from aviation by 26.8%. Complete desulfurisation of aviation fuel reduces the global aerosol burden
 458 from aviation by 28.4%, with the global sulfate burden from aviation reduced by 71.6% (Table 3). When
 459 aviation emissions contain no sulfur, aviation-induced sulfate is formed through aviation NO_x-induced
 460 increases in OH concentrations, resulting in the oxidation of SO₂ from non-aviation sources (Unger et al., 2006;
 461 Barrett et al., 2010).

462

463 **Table 3: Global aviation-induced aerosol mass burdens for different emission scenarios. Values in**
 464 **parentheses show percentage change relative to NORM case.**

Scenario	All components (Gg)	Sulfates (Gg)	Nitrates (Gg)
NORM	16.9	12.9	5.7
ULSJ	12.4 (–26.8%)	4.0 (–69.1%)	5.9 (+4.5%)
DESUL	12.1 (–28.4%)	3.7 (–71.6%)	6.0 (+5.1%)
No NO _x and SO ₂	2.0 (–88.3%)	0.3 (–97.5%)	0.1 (–97.9%)

465

466 In line with previous work, we find a substantial fraction of aviation sulfate can be attributed to aviation NO_x
 467 emissions and not directly to aviation SO₂ emissions. We estimate that 36% aviation-attributable sulfates
 468 formed at the surface are associated with aviation NO_x emissions, compared to ~63% estimated by Barrett et
 469 al. (2010) using the GEOS-Chem model (both estimates for FSC = 600 ppm). Differences between model
 470 estimates can be attributed to differences in model chemistry and microphysics, and different aviation NO_x
 471 emissions. We find desulfurisation increases the aviation nitrate burden by 5.1% (Table 3); although much of
 472 this increase occurs at altitudes well above the surface (Fig. 5) and so is not reflected in surface PM_{2.5}
 473 concentrations.

474

475 We explored the impacts of NO_x emission reductions in combination with fuel desulfurisation. A scenario with
 476 desulfurised fuel and zero NO_x emissions reduces the global aviation-induced aerosol burden by 88.3% (Table
 477 3), in comparison to a desulfurised only case (DESUL), where the aviation-induced aerosol burden is reduced
 478 by 28.4%. Removal of aviation NO_x and SO₂ emissions results in a 95.0% reduction in aviation-induced global
 479 mean surface level aviation-induced PM_{2.5}. These results imply that only limited sulfate reductions can be

480 achieved through reducing FSC alone, with further reductions in aviation-induced PM_{2.5} sulfates requiring
481 additional controls on aviation NO_x emissions.
482

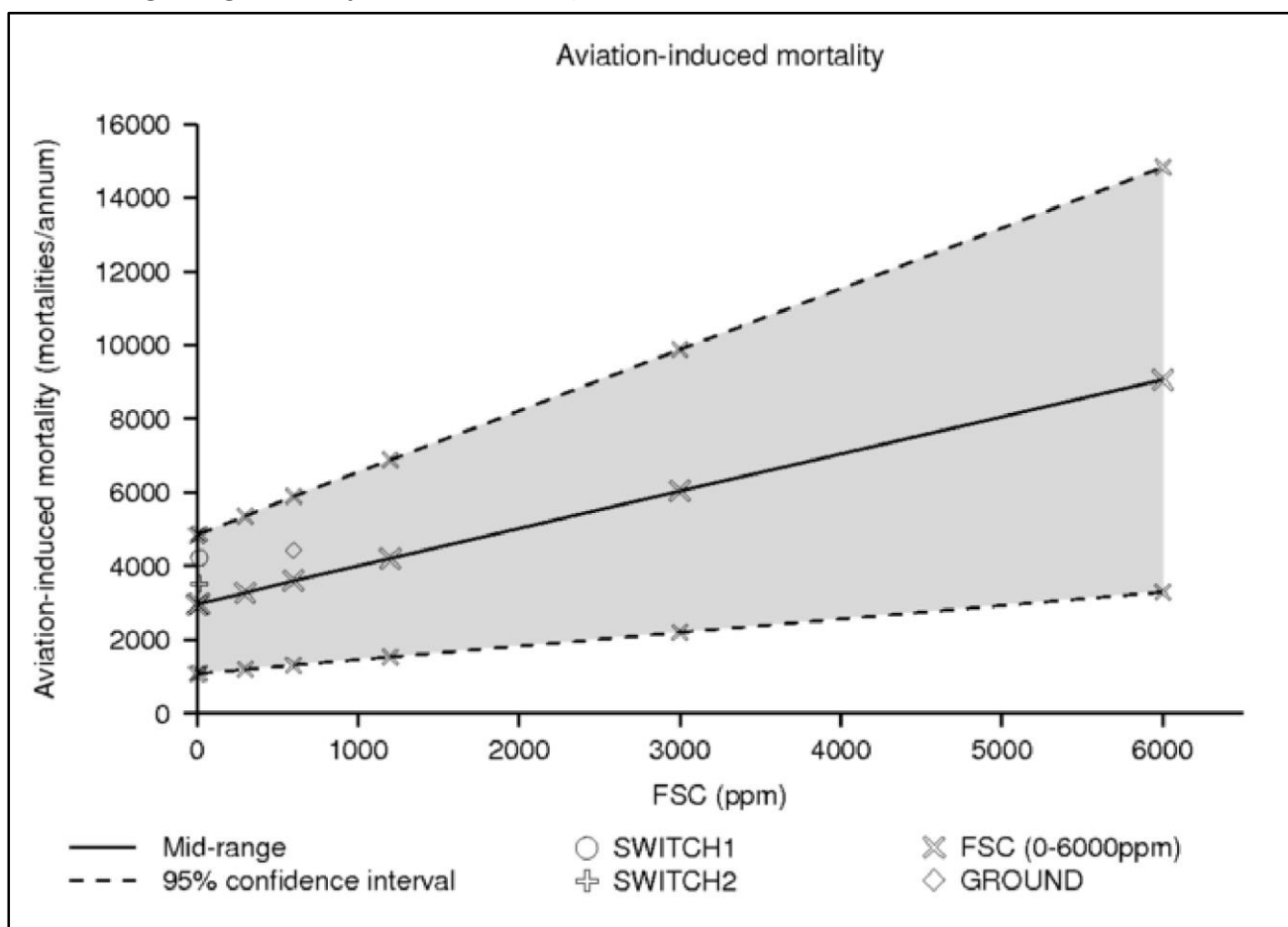
483 **3.2 Premature mortality**

484 Fig. 6 shows estimated annual premature mortalities (from cardiopulmonary disease and lung cancer) due to
485 aviation-induced changes in PM_{2.5} as a function of FSC. We estimate that aviation emissions with standard FSC
486 (FSC = 600 ppm) cause 3,600 [95% CI: 1,310–5,890] premature mortalities each year, with 3210 [95% CI: 1160–
487 5250] mortalities a⁻¹ due to increases in cases of cardiopulmonary disease and 390 [95% CI: 150–640]
488 mortalities a⁻¹ due to increases in cases of lung cancer. Low-, mid- and high-range cause-specific coefficients
489 (β) are used to account for uncertainty in the health impacts caused by exposure to PM_{2.5} (Section 2.5) (Ostro,
490 2004). Our estimated global mortality due to aviation emissions is greatest in the Northern Hemisphere, which
491 accounts for 98.7% of global mortalities. Europe and North America account for 42.3% and 8.4% of mortality
492 due to aviation emissions respectively.
493

494 Our estimate of the premature mortality due to aviation lies within the range of previous estimates (310–
495 13,920 mortalities a⁻¹) (Barrett et al., 2010; Barrett et al., 2012; Jacobson et al., 2013; Morita et al., 2014; Yim
496 et al., 2004). Barrett et al. (2012) estimated ~10,000 mortalities a⁻¹ due to aviation, almost a factor 3 higher
497 than our central estimate. The greater aviation-induced mortality simulated by Barrett et al. (2012), can be
498 attributed to greater aviation-induced surface PM_{2.5} concentrations simulated in their study, particularly over
499 highly populated areas. Their study simulated maximum aviation-induced PM_{2.5} concentrations over Europe,
500 eastern China and eastern North America greater than those in our simulations by factors of 5 for Europe and
501 eastern China and 2.5 over eastern North America. Our aviation-induced sulfate concentrations compare well
502 with Barrett et al. (2012), indicating that the resulting differences in aviation-induced surface PM_{2.5}
503 concentrations are a result of other aerosol components. Additionally, differences in mortality arise due to the
504 use of different cause-specific coefficients (β) within the same CRF, as well as different population datasets.
505 Morita et al. (2014) estimate that aviation is responsible for 405 [95% CI: 182–648] mortalities a⁻¹. This lower
506 estimate is primarily due to the mortality functions used, with Morita et al. (2014) using the integrated
507 exposure response (IER) function as described by Burnett et al. (2014). The IER function considers a PM_{2.5}
508 concentration below which there is no perceived risk, reducing estimated impacts of aviation in regions of low
509 PM_{2.5} concentrations.
510

511
512
513
514
515
516
517
518
519
520
521
522
523
524
525
526
527
528
529
530
531
532

533 **Fig. 6: Estimated global aviation-induced mortality as a function of FSC, and changes in vertical aviation-**
 534 **emissions distributions for year 2000 (Shaded region denotes the 95% confidence through application of**
 535 **low- and high-range cause-specific coefficients).**



536 We estimate that aviation emissions with ULSJ fuel result in 2,970 [95% CI: 1,080–4,870] premature mortalities
 537 globally per annum. Therefore, changing from standard FSC to ULSJ would result in 620 [95% CI: 230–1,020]
 538 fewer premature mortalities globally per annum; a reduction in aviation-induced mortalities of 17.4%.
 539 Regionally we find the implementation of an ULSJ fuel reduces annual mortality by 180 over Europe and by
 540 110 over North America.

541
 542 Barrett et al. (2012) estimated that swapping to ULSJ fuel could result in ~2,300 [95% CI: 890–4,200] fewer
 543 premature mortalities globally per annum; a reduction of 23%. In their work (using GEOS-Chem), the use of
 544 ULSJ reduces global mean PM_{2.5} concentrations (sulfates, nitrates and ammonium) by 0.89 ng m⁻³, less than
 545 the 1.61 ng m⁻³ reduction in PM_{2.5} simulated here). Despite the greater reductions in global mean surface layer
 546 PM_{2.5} concentrations simulated here, Barrett et al. (2012) simulate greater reductions in PM_{2.5} over populated
 547 regions, resulting in greater reductions of aviation-induced mortality under the ULSJ scenario. Additionally,
 548 the GRUMPv1 population dataset that Barrett et al. (2012) use resolves population data on a finer scale
 549 compared to the resolution of GPWv3 population dataset used here (Center for International Earth Science
 550 Information Network, 2012); differences which could contribute to differences in estimates of mortality.

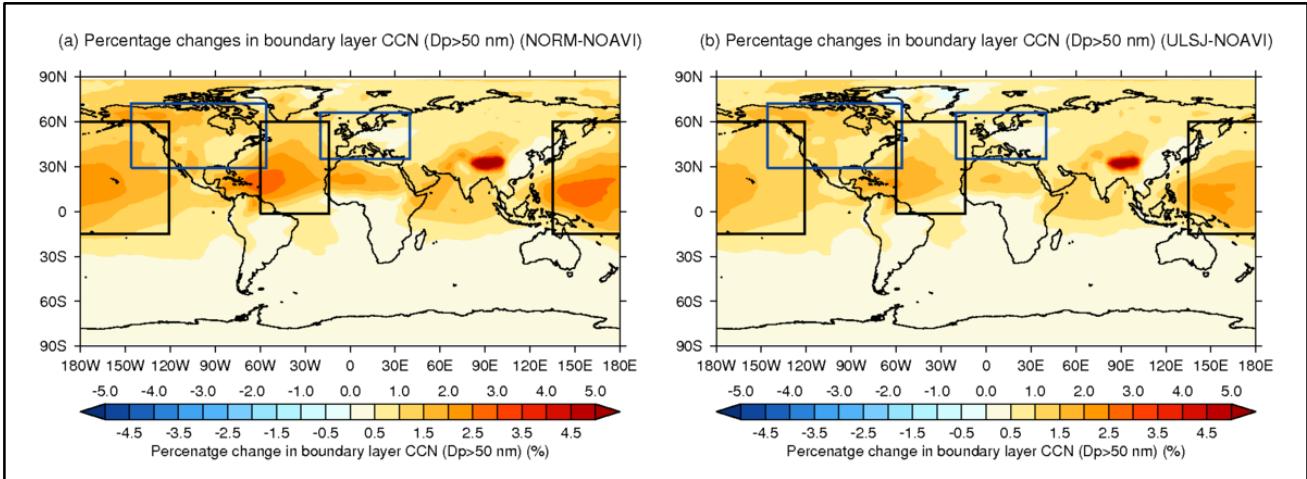
551
 552 We also estimate how aviation-induced mortality would change if FSC was increased. We find that increasing
 553 FSC to 3000 ppm (HIGH) would increase annual aviation-induced mortalities to 6,030, an increase of 67.8%
 554 in relation to standard aviation (NORM; FSC = 600 ppm).
 555

556 3.3 Sensitivity of cloud condensation nuclei to aviation FSC

557 Aviation emissions with standard FSC (NORM; FSC = 600 ppm) increase global annual mean cloud condensation
 558 nuclei (CCN), here taken as the number of soluble particles with a dry diameter greater than 50 nm, at low-

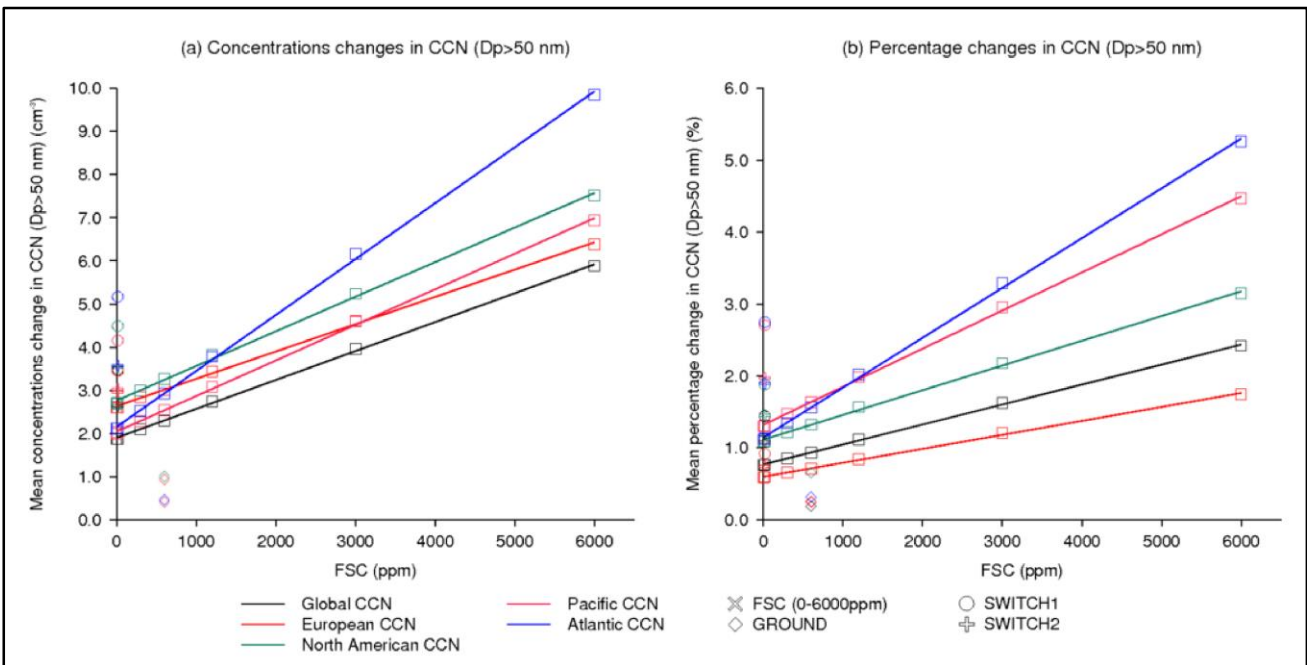
559 cloud level (879hPa; 0.96km) by 0.9% (2.3 cm^{-3}) (Fig. 7(a)). Increases in CCN concentrations are greater in the
 560 Northern Hemisphere [$+3.9 \text{ cm}^{-3}$; $+1.4\%$] compared to the Southern Hemisphere [$+0.7 \text{ cm}^{-3}$; $+0.5\%$]. Maximum
 561 increases in low-level CCN are simulated over the Pacific, central Atlantic and Arctic Oceans.

562
 563 **Fig. 7: Impact of aviation emissions on low-cloud level (879 hPa) CCN ($D_p > 50 \text{ nm}$) concentrations: (a)**
 564 **standard FSC (NORM–NOAVI) and (b) FSC = 15 ppm (ULSJ–NOAVI). Blue boxes define North American and**
 565 **European regions, and black boxes define Atlantic (60°W – 14°W , 1.4°S – 60°N) and Pacific regions (135°E –**
 566 **121°W , 15°S – 60°N) referred to in the text.**



567 The use of ULSJ (FSC = 15 ppm) reduces global mean low-level CCN concentrations by 0.4 cm^{-3} , [-18.2%]
 568 relative to the NORM case (Fig. 7). Northern Hemisphere CCN concentrations are reduced by 0.8 cm^{-3} [-19.4%],
 569 while Southern Hemisphere concentrations are reduced by 0.1 cm^{-3} [-11.5%] (Fig. 7).

570
 571 **Fig. 8: Global and regional variations in low-cloud level (879 hPa) CCN ($D_p > 50 \text{ nm}$): (a) changes in mean**
 572 **concentrations and (b) percentage changes. See Fig. 5 for definitions of regions.**



573 Fig. 8 shows the sensitivity of low level CCN concentrations to FSC. As with $\text{PM}_{2.5}$, we find simulated changes
 574 in CCN are near linear with respect to FSC ($R^2 > 0.99$ and p -value < 0.001 globally and for all individual regions).
 575

576 ULSJ fuel reduces global mean CCN by -0.42 cm^{-3} with largest reductions over the Atlantic Ocean [-0.81 cm^{-3}],
 577 North America [-0.55 cm^{-3}], and the Pacific Ocean [-0.51 cm^{-3}], i.e. in relation to standard aviation (ULSJ–
 578 NORM). The complete desulfurisation of aviation fuel results in reductions in CCN in relation to standard
 579 aviation (DESUL–NORM), which follow the same regional trends (Fig. 8(a)).

580

581 3.4 Sensitivity of aerosol and ozone radiative effect to FSC

582

583 Fig. 9 shows the calculated global mean net RE due to non-CO₂ aviation emissions. For standard FSC (FSC = 600
584 ppm) emissions the global mean combined RE is -13.3 mW m^{-2} . This combined radiative effect (RE_{comb}) results
585 from a balance between a positive aDRE of $+1.4 \text{ mW m}^{-2}$ and O3DRE $+8.9 \text{ mW m}^{-2}$, and a negative aCAE of $-$
586 23.6 mW m^{-2} (Fig. 9).

587

588 Our estimated aviation aerosol DRE [$+1.4 \text{ mW m}^{-2}$] lies in the middle of the range given by previous work. The
589 aviation aerosol DRE has been previously assessed as highly uncertain, ranging between -28 to $+20 \text{ mW m}^{-2}$
590 (Righi et al., 2013). Our estimated aviation-induced aCAE [-23.6 mW m^{-2}] lies within the range of uncertainty
591 from previous literature: Righi et al. (2013) estimated $-15.4 \pm 10.6 \text{ mW m}^{-2}$ and Gettelman and Chen (2013)
592 estimated $-21 \pm 11 \text{ mW m}^{-2}$.

593

594 Our O3DRE estimate ($+8.9 \text{ mW m}^{-2}$), normalised by global aviation NO_x emission to $+10.5 \text{ mW m}^{-2} \text{ Tg(N)}^{-1}$, is at
595 the lower end of current estimates [$7.4\text{--}37.0 \text{ mW m}^{-2} \text{ Tg(N)}^{-1}$] (Sausen et al., 2005; Köhler et al., 2008; Hoor et
596 al., 2009; Lee et al., 2009; Holmes et al., 2011; Myhre et al., 2011; Unger, 2011; Frömming et al., 2012; Skowron
597 et al., 2013; Unger et al., 2013; Khodayari et al., 2014). This can be attributed to the lower net O₃ chemical
598 production efficiency (OPE) within our model (1.33). Unger (2011) estimated an O3DRE of $7.4 \text{ mW m}^{-2} \text{ Tg(N)}^{-1}$
599 with a model OPE of ~ 1 , while the ensemble of models considered by Myhre et al. (2011) have an OPE range
600 of 1.5–2.4, resulting in an O3DRE range of 16.2–25.4 $\text{mW m}^{-2} \text{ Tg(N)}^{-1}$.

601

602 We calculate that an aviation fleet utilising ULSJ fuel would result in a in a global annual mean RE_{comb} of -6.3
603 mW m^{-2} [aDRE = $+1.8 \text{ mW m}^{-2}$; aCAE = -16.8 mW m^{-2} ; and O3DRE = $+8.7 \text{ mW m}^{-2}$]. Thus, swapping from
604 standard aviation fuel to ULSJ fuel reduces the net cooling effect from aviation-induced aerosol and O₃ by 7.0
605 mW m^{-2} , in comparison to the reduction of 3.3 mW m^{-2} estimated by Barrett et al. (2012). In our model, this
606 change is primarily due a reduction in cooling from the aCAE of $+6.7 \text{ mW m}^{-2}$ combined with smaller
607 contributions from an increased aDRE of $+0.4 \text{ mW m}^{-2}$, and reduction in warming from the O3DRE of -0.12
608 mW m^{-2} (Fig. 9).

609

610 When we assume fully desulfurised aviation jet fuel (DESUL; FSC = 0 ppm), the RE_{comb} induced by aviation-
611 induced aerosol and O₃ is very similar to that for ULSJ fuel and is estimated as -6.1 mW m^{-2} [aDRE = $+1.8 \text{ mW}$
612 m^{-2} ; aCAE = -16.6 mW m^{-2} ; and O3DRE = $+8.7 \text{ mW m}^{-2}$].

613

614

615

616

617

618

619

620

621

622

623

624

625

626

627

628

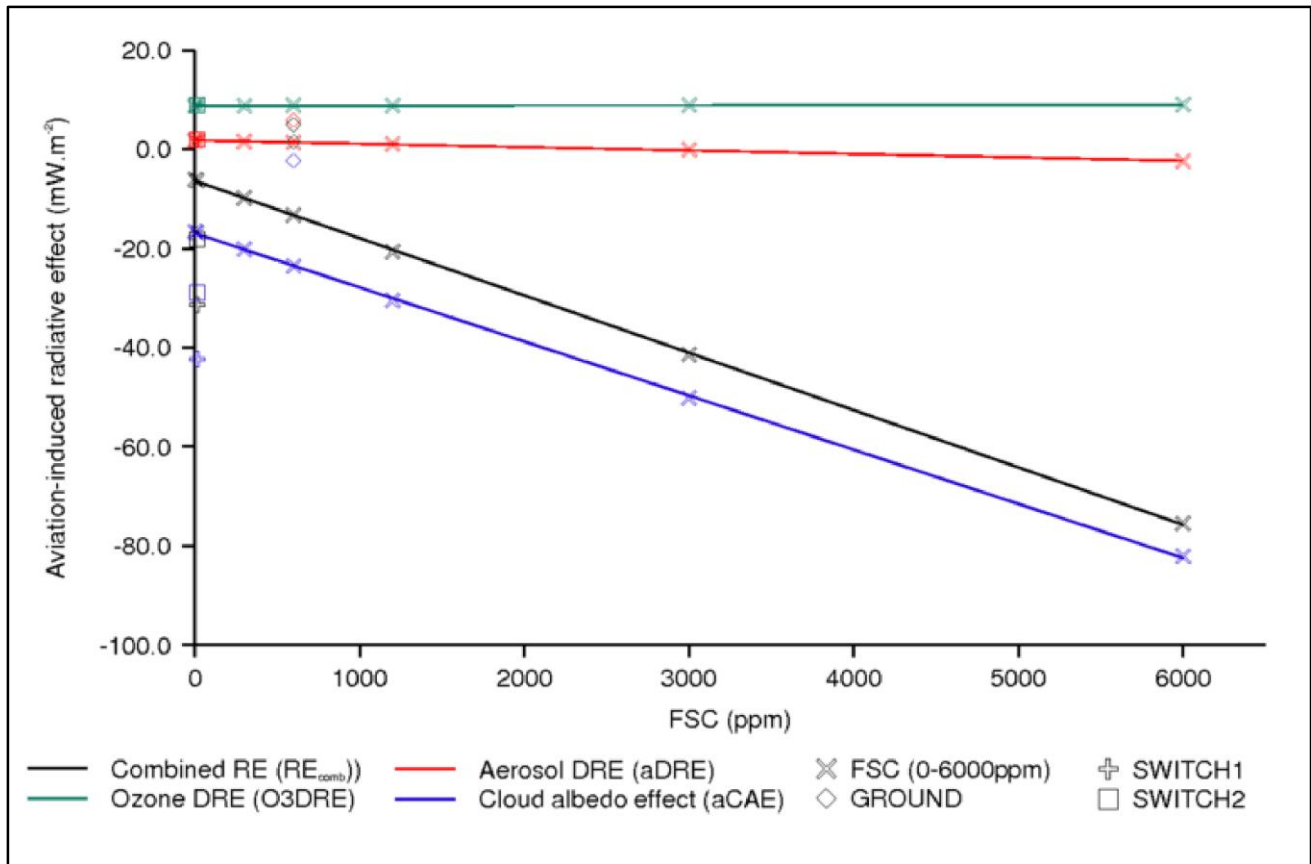
629

630

631

632

633 **Fig. 9: Aviation-induced radiative effects due to variations in fuel sulfur content (FSC), the ground release of**
 634 **aviation emissions (GROUND), and variations in the vertical distribution of aviation SO₂ emissions (SWITCH1**
 635 **and SWITCH2 simulations).**

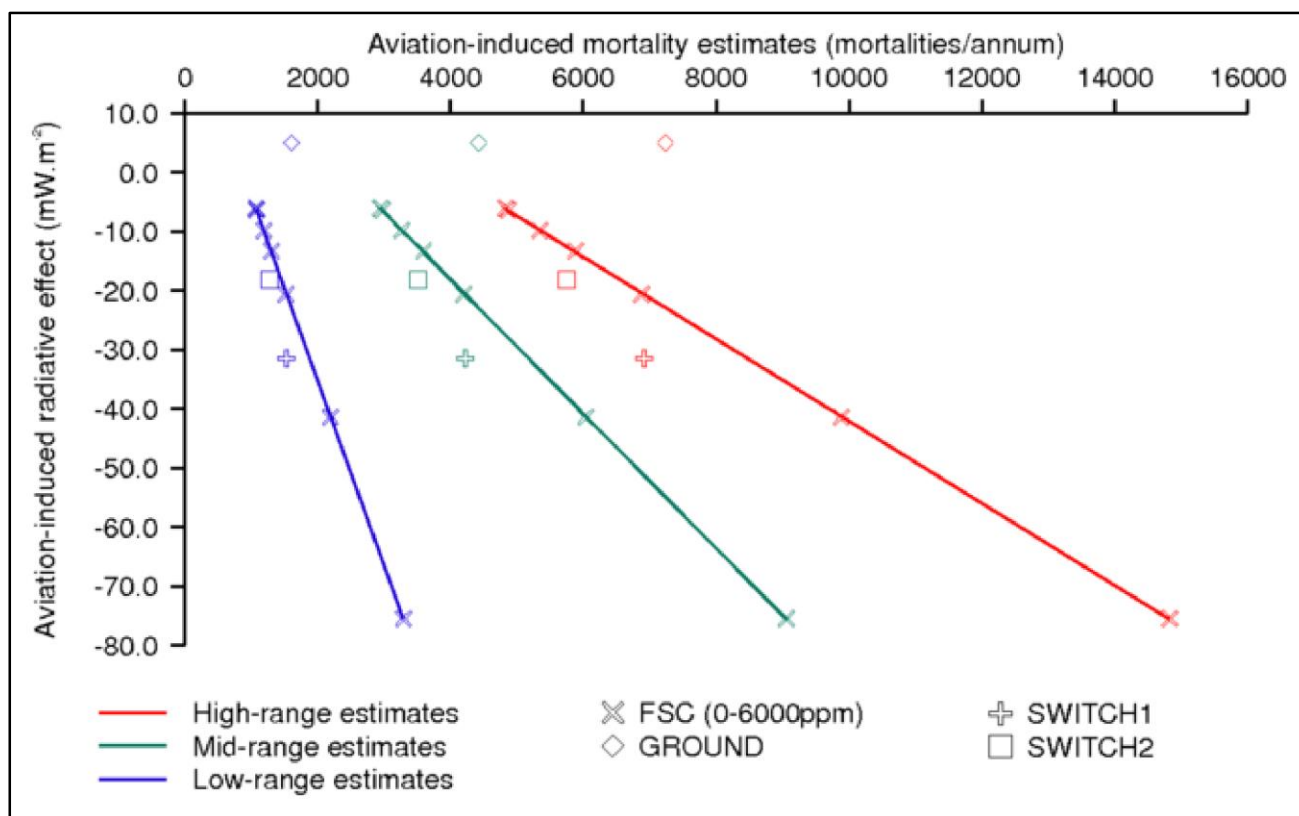


636 Increases in FSC result in reductions in the aerosol DRE (aDRE), changing from a positive aerosol DRE for low
 637 FSC scenarios, to a negative aerosol DRE for high FSC (FSC > 1200 ppm). As FSC is increased, we find the aCAE
 638 exhibits a larger cooling effect, i.e. becoming more negative with increases in FSC, increasing by a factor ~5 as
 639 FSC is increased from 0 to 6000 ppm. The RE_{comb} is dominated by these changes to the aCAE. As a result
 640 increases in FSC from 0–6000 ppm, result in a greater negative (cooling) aviation-induced RE_{comb}; increasing in
 641 magnitude by a factor of ~5 (–16.6 mW m⁻² for FSC = 0 ppm to –82.1 mW m⁻² for FSC = 6000 ppm) (Fig. 9).
 642 Therefore, we find that increases in FSC provide a cooling effect due to the dominating effect from aviation-
 643 induced aCAE.
 644

645 3.5 Relationship between aviation-induced radiative effects and mortality due to aviation 646 non-CO₂ emissions

647 Fig. 10 shows the net RE and premature mortality for different aviation emission scenarios. Increases in FSC
 648 lead to approximately linear increases in both estimated mortality and the negative net RE. We quantify the
 649 impact of FSC on mortality and REs in terms of d(mortalities)/d(FSC) [mortalities ppm⁻¹] and d(RE)/d(FSC) [mW
 650 m⁻² ppm⁻¹]. We calculate the sensitivity of global premature mortality to be 1.0 mortalities ppm⁻¹ [95% CI = 0.4
 651 to 1.6 mortalities ppm⁻¹, where the range is due to uncertainty in β]. The global mean RE_{comb} has a sensitivity
 652 of –1.2x10⁻² mW m⁻² ppm⁻¹, dominated by large changes to the aCAE [–1.1x10⁻² mW m⁻² ppm⁻¹], and much
 653 smaller changes in the aDRE [–6.9x10⁻⁴ mW m⁻² ppm⁻¹] and O₃ RE [+4.4x10⁻⁵ mW m⁻² ppm⁻¹].
 654
 655
 656
 657
 658
 659
 660

661 **Fig. 10: Relationship between net radiative effect [sum of ozone direct (O3DRE), aerosol direct radiative**
 662 **(aDRE) and aerosol cloud albedo (aCAE) effects] and annual mortality rates: for low- mid- and high-range**
 663 **mortality sensitivities.**



664 The different slopes in the relationship between estimated RE and mortality (Fig. 10) are driven by the range
 665 of coefficients used in the CRF. This highlights the considerable uncertainty in the health impacts caused by
 666 exposure to PM_{2.5}. We note that uncertainty in the RE due to aerosol and ozone exists, but is not included in
 667 Fig. 9.

668
 669 To assess how the vertical distributions of aviation SO₂ emissions influence human health and climate effects,
 670 we performed three additional simulations where we altered the vertical distribution of aviation SO₂ emissions
 671 (GROUND, SWITCH1 and SWITCH2 simulations). In these simulations the relationships between mortality and
 672 net RE deviate from the linear relationship seen when varying FSC between 0–6000 ppm (Fig. 10).

673
 674 In relation to the standard aviation emissions simulation (FSC = 600 ppm; NORM), when we release all aviation
 675 emissions at the surface (GROUND; FSC = 600 ppm) aviation-induced surface PM_{2.5} concentrations increase by
 676 +13.5 ng m⁻³ [+65.7%] over Europe and by +1.7 ng m⁻³ [+27.1%] over North America, but decrease by -1.4 ng
 677 m⁻³ [-36.7%] globally (Fig. 4). Greater surface layer PM_{2.5} perturbations (GROUND–NORM) over populated
 678 regions increase aviation-induced annual mortality by +22.9% [+830 mortalities a⁻¹] (Fig. 6).

679
 680 Releasing aviation emissions at the surface (GROUND case) increases global mean cloud level CCN by only 0.4
 681 cm⁻³ relative to NOAVI; providing a reduction in CCN of 82.1% [-1.89 cm⁻³] relative to the NORM case (i.e.
 682 GROUND–NORM). That is, injecting aviation emissions into the free troposphere in the standard scenario is
 683 over 5 times more efficient at increasing CCN concentrations compared to when the same emissions are
 684 released at the surface [GROUND CCN = 0.4 cm⁻³; NORM CCN = 2.3 cm⁻³]; both in relation to the NOAVI
 685 scenario. Similar behaviour has been demonstrated previously for volcanic SO₂ emissions by Schmidt et al.
 686 (2012), where volcanic SO₂ emissions injected into the free troposphere (FT) were more than twice as effective
 687 at producing new CCN compared to boundary layer emissions of DMS. Injection of aviation SO₂ emissions at
 688 the surface will increase both deposition rates and aqueous phase oxidation of SO₂; the latter resulting in the
 689 growth of existing CCN, but not the formation of new CCN. In contrast, when SO₂ is emitted into the FT the
 690 dominant oxidation mechanism is to H₂SO₄, leading to the formation of new CCN through particle formation

691 and the condensational growth of particles to larger sizes. Subsequent entrainment of these new particles into
692 the lower atmosphere results in enhanced CCN concentrations in low level clouds. Reduced CCN formation
693 when aviation emissions are injected at the surface has implications for the aCAE. When aviation emissions
694 are released at the surface we calculate an aCAE of -2.3 mW m^{-2} ; a factor of 10 smaller than the standard
695 aviation scenario. This demonstrates that low-level CCN concentrations and the aCAE are particularly sensitive
696 to aviation emissions, because of the efficient formation of CCN when SO_2 emissions are injected into the FT.
697 Injecting aviation emissions at the surface also results in an increase in the aDRE of $+5.9 \text{ mW m}^{-2}$, resulting in
698 a RE_{comb} of $+5.0 \text{ mW m}^{-2}$ (Fig. 9).

700 Surface O_3 concentrations are also less sensitive to aviation when emissions are located at the surface. Global
701 mean aviation-induced surface O_3 concentrations are reduced from 0.15 ppbv (NORM) to 0.03 ppbv when all
702 emissions are in the surface layer. Releasing aviation emissions at the surface also reduces the global O_3
703 burden by 3.1 Tg. These perturbations in O_3 concentrations result in a reduction in the O_3 radiative effect from
704 $+8.9 \text{ mW m}^{-2}$ (NORM; FSC = 600 ppm) to $+1.5 \text{ mW m}^{-2}$ (GROUND; FSC = 600 ppm) (Fig. 9). This is a reflection
705 of increases in the OPE of NO_x with increases in altitude due to lower background NO_x and NMHC (non-
706 methane hydrocarbon) concentrations (Köhler et al., 2008; Stevenson and Derwent, 2009; Snijders and
707 Melkers, 2011; Skowron et al., 2013).

709 We investigated altering FSC between the take-off / landing and the cruise phases of flight using two scenarios
710 (SWITCH1 and SWITCH2) (Table 2). Our SWITCH1 scenario increases global mean aviation-induced surface
711 layer $\text{PM}_{2.5}$ concentrations by $+2.1 \text{ ng m}^{-3}$ [52.2%], European mean concentrations by $+0.9 \text{ ng m}^{-3}$ [+4.5%], and
712 North American concentrations by $+2.7 \text{ ng m}^{-3}$ [+42.2%] relative to NORM (Fig. 4). These changes increase
713 aviation-induced mortality by $+17.4\%$ [+630 mortalities a^{-1}] (Fig. 6). This scenario results in greater global mean
714 increases in CCN (relative to NORM) of $+1.2 \text{ cm}^{-3}$ [+51.2%], a larger cooling aCAE [-42.4 mW m^{-2}], larger
715 warming aDRE [2.07 mW m^{-2}], resulting in additional -18.1 mW m^{-2} [136%] of aviation-induced cooling
716 [SWITCH1 RE_{comb} of -31.4 mW m^{-2}].

718 The SWITCH2 scenario was designed to have the same global total sulfur emission as the normal aviation
719 simulation. SWITCH2 increased global mean surface aviation-induced $\text{PM}_{2.5}$ concentrations by $+0.3 \text{ ng m}^{-3}$
720 [+6.6%], but reduces mean surface $\text{PM}_{2.5}$ concentrations over Europe [-1.8 ng m^{-3} ; -8.7%] and North America
721 [-0.8 ng m^{-3} ; -12.8%] compared to NORM. Under this scenario global aviation-induced mortality is decreased
722 by 2.4% [-90 mortalities a^{-1}] compared to the standard aviation simulation (Fig. 6). The SWITCH2 scenario
723 results in a RE_{comb} of -18.2 mW m^{-2} , providing an additional -4.9 mW m^{-2} [36.6%] cooling in relation to standard
724 aviation emissions (NORM; FSC = 600 ppm).

725

726 4 Discussion and Conclusions

727 We have used a coupled chemistry-aerosol microphysics model to estimate the impact of aviation emissions
728 on aerosol and O_3 concentrations, premature mortality and radiative effect on climate.

729

730 We calculated the top-of-atmosphere (TOA) tropospheric O_3 radiative effect (O3DRE), aerosol direct RE (aDRE)
731 and aerosol cloud albedo effect (aCAE). We find that these non- CO_2 REs result in a net cooling effect on climate
732 as has been found previously (Sausen et al., 2005; Lee et al., 2009; Gettelman and Chen, 2013; Righi et al.,
733 2013; Unger et al., 2013). For year 2000 aviation emissions with a standard fuel sulfur content (FSC = 600 ppm),
734 we calculate a global annual mean net TOA RE of -13.3 mW m^{-2} , due to a combination of O3DRE [$+8.9 \text{ mW m}^{-2}$],
735 aDRE [$+1.4 \text{ mW m}^{-2}$] and aCAE [-23.6 mW m^{-2}].

736

737 Our O3DRE [$+8.9 \text{ mW m}^{-2}$] when normalised to represent the impact of the emissions of 1Tg(N) [$+10.45 \text{ mW}$
738 $\text{m}^{-2} \text{ Tg(N)}^{-1}$] is at the lower end of range provided by previous studies [$7.39\text{--}36.95 \text{ mW m}^{-2} \text{ Tg(N)}^{-1}$] (Sausen et
739 al., 2005; Hoor et al., 2009; Lee et al., 2009; Holmes et al., 2011; Myhre et al., 2011; Unger, 2011; Frömming
740 et al., 2012; Unger et al., 2013; Khodayari et al., 2014). This can be attributed to our model's lower OPE of
741 1.33, in comparison to the range of 1–2.4 from other models (Myhre et al., 2011; Unger, 2011).

742

743

744 Our estimate of aviation-induced aCAE [-23.6 mW m^{-2}] lies just outside the range provided by Gettelman and
745 Chen (2013) and Righi et al. (2013) [-15.4 to -21 mW m^{-2}]. Our estimated aDRE [$+1.4 \text{ mW m}^{-2}$] lies within the
746 middle of the range given by previous work (Sausen et al., 2005; Fuglestedt et al., 2008; Lee et al., 2009;
747 Balkanski et al., 2010; Unger, 2011; Gettelman and Chen, 2013; Righi et al., 2013; Unger et al., 2013).

748
749 We estimate that standard aviation (NORM; FSC = 600 ppm) is responsible for approximately 3,600 premature
750 mortalities annually due to increased surface layer $\text{PM}_{2.5}$, in line with previous work (Barrett et al., 2012). We
751 find that aviation-induced mortalities are highest over Europe, eastern North America and eastern China;
752 reflecting larger regional perturbations in surface layer $\text{PM}_{2.5}$ concentrations. Comparing these estimates with
753 total global premature mortalities from ambient air pollution from all anthropogenic sources (Lim et al., 2012),
754 aviation is responsible for 0.1% [0.04–0.18%] of annual premature mortalities.

755
756 We investigated the impact of varying aviation FSC over the range 0–6000 ppm. Increases in FSC lead to
757 increases in surface $\text{PM}_{2.5}$ concentrations and subsequent increases in aviation-induced mortality. Increases in
758 FSC also lead to a more negative RE_{comb} due to an enhanced aCAEs. We estimate that the use of ultra-low sulfur
759 jet (ULSJ) fuel, with a FSC of 15 ppm, could prevent 620 [230–1,020] mortalities annually compared to standard
760 aviation emissions. Swapping to ULSJ fuel increases the global mean net RE by $+7.0 \text{ mW m}^{-2}$ compared to
761 standard aviation emissions, largely due to a reduced aCAE. We calculate a larger warming effect from
762 switching to ULSJ fuel than that assessed by Barrett et al. (2012), who did not evaluate changes in aCAE.

763
764 Absolute reductions in FSC result in limited reductions in aviation-induced surface layer $\text{PM}_{2.5}$. We estimate
765 that aviation- NO_x emissions are responsible for 36.2% of aviation-induced sulfate perturbations. Thus further
766 reductions in aviation-induced $\text{PM}_{2.5}$ can potentially be achieved if NO_x emission reductions are implemented
767 in tandem with reductions to fuel sulfur content.

768
769 In line with previous work (Köhler et al., 2008; Stevenson and Derwent, 2009; Snijders and Melkers, 2011;
770 Frömming et al., 2012; Skowron et al., 2013), decreasing the altitude at which O_3 forming species are emitted
771 results in a reduction in aviation-induced O_3 , and resulting O3DRE. This is due to the relationship between
772 altitude and OPE, and the inverse relationship between altitude and background pollutant concentrations. We
773 also explored the sensitivity of emission injection altitude on aerosol, mortality and aerosol RE. Injecting
774 aviation emissions at the surface results in a reduction in global mean concentrations of $\text{PM}_{2.5}$ (relative to
775 NORM), but with higher regional concentrations over central Europe and eastern America; resulting in higher
776 annual mortalities due to aviation. We find that aviation emissions are a factor of 5 less efficient at creating
777 CCN when released at the surface, resulting in an aCAE of -2.3 mW m^{-2} , a reduction of 90.1% in relation to the
778 standard aviation scenario. When aviation SO_2 emissions are injected into the free-troposphere, the dominant
779 oxidation pathway is to H_2SO_4 followed by particle formation and condensational growth of new particles to
780 larger sizes. Subsequent entrainment of these new particles into the lower atmosphere leads to increased CCN
781 concentrations and impacts on cloud albedo. Aviation SO_2 emissions are therefore particularly efficient at
782 forming CCN with resulting impacts on cloud albedo.

783
784 We explored the impact of applying altitude dependent variations in aviation FSC. We tested a scenario with
785 high FSC in the free troposphere and low FSC near the surface, resulting in the same global aviation sulfur
786 emission as the standard aviation scenario. In this scenario, aviation-induced premature mortalities were
787 reduced by 2.4% [-90 mortalities a^{-1}] and the magnitude of the negative RE_{comb} was increased by 36.6%,
788 providing an additional cooling impact of climate of -4.88 mW m^{-2} .

789
790 Our simulations suggest that the climate and air quality impacts of aviation are sensitive to FSC and the altitude
791 of emissions. We explored a range of scenarios to maximise climate cooling and reduce air quality impacts.
792 Use of ULSJ fuel (FSC = 15 ppm) at low altitude combined with high FSC in the free troposphere results in
793 increased climate cooling whilst reducing aviation mortality. More complicated emission patterns, for
794 example, use of high FSC only whilst over oceans might further enhance this effect. However, we note that
795 the greatest reduction in aviation-induced mortality is simulated for complete desulfurisation of aviation fuel.
796 Given the uncertainty in both the climate and air quality impacts of aerosol and ozone, additional simulations
797 from a range of atmospheric models are required to explore the robustness of our calculations. Finally, we

798 note that our calculations are limited to calculation of aviation-induced RE. Future work needs to assess the
799 complex climate impacts of altering aviation FSC. Future work needs to estimate the health impacts of aviation
800 using newly available concentration response functions (Burnett et al., 2014).
801

802 **Author information**

803 *Phone: 0113 343 8167. E-mail: pm08zzk@leeds.ac.uk
804

805 **Acknowledgements**

806 The authors acknowledge the Engineering & Physical Sciences Research Council (EPSRC) for funding of Z Z
807 Kapadia through the EPSRC Doctoral Training Centre in Low Carbon Technologies (EPSRC Grant
808 EP/G036608/1).
809

810 The authors are also grateful to Jean-Francois Lamarque and the 'Historical emissions group' and IIASA for
811 their publically available recommended historical CMIP5 aviation emissions data.
812

813 **References**

- 814 Airbus: A318/A319/A320/A321 FCTM (Flight Crew Training Manual), FCA A318/A319/A320/A321 FLEET,
815 2008.
- 816 Anderson, B. E., Chen, G., and Blake, D. R.: Hydrocarbon emissions from a modern commercial airliner,
817 *Atmospheric Environment*, 40, 3601-3612, <http://dx.doi.org/10.1016/j.atmosenv.2005.09.072>, 2006.
- 818 Andres, R. J., and Kasgnoc, A. D.: A time-averaged inventory of subaerial volcanic sulfur emissions, *Journal of*
819 *Geophysical Research: Atmospheres*, 103, 25251-25261, 10.1029/98JD02091, 1998.
- 820 Arnold, S. R., Chipperfield, M. P., and Blitz, M. A.: A three-dimensional model study of the effect of new
821 temperature-dependent quantum yields for acetone photolysis, *Journal of Geophysical Research:*
822 *Atmospheres*, 110, D22305, 10.1029/2005JD005998, 2005.
- 823 ASTM International: D1655-11b: Standard Specification for Aviation Turbine Fuels, ASTM International, West
824 Conshohocken, PA, United States, 2012.
- 825 Balkanski, Y., Myhre, G., Gauss, M., Rädcl, G., Highwood, E. J., and Shine, K. P.: Direct radiative effect of
826 aerosols emitted by transport: from road, shipping and aviation, *Atmos. Chem. Phys.*, 10, 4477-4489,
827 10.5194/acp-10-4477-2010, 2010.
- 828 Barahona, D., West, R. E. L., Stier, P., Romakkaniemi, S., Kokkola, H., and Nenes, A.: Comprehensively
829 accounting for the effect of giant CCN in cloud activation parameterizations, *Atmos. Chem. Phys.*, 10, 2467-
830 2473, 10.5194/acp-10-2467-2010, 2010.
- 831 Barrett, S. R. H., Britter, R. E., and Waitz, I. A.: Global Mortality Attributable to Aircraft Cruise Emissions,
832 *Environmental Science & Technology*, 44, 7736-7742, 10.1021/es101325r, 2010.
- 833 Barrett, S. R. H., Yim, S. H. L., Gilmore, C. K., Murray, L. T., Kuhn, S. R., Tai, A. P. K., Yantosca, R. M., Byun, D.
834 W., Ngan, F., Li, X., Levy, J. I., Ashok, A., Koo, J., Wong, H. M., Dessens, O., Balasubramanian, S., Fleming, G.
835 G., Pearlson, M. N., Wollersheim, C., Malina, R., Arunachalam, S., Binkowski, F. S., Leibensperger, E. M.,
836 Jacob, D. J., Hileman, J. I., and Waitz, I. A.: Public Health, Climate, and Economic Impacts of Desulfurizing Jet
837 Fuel, *Environmental Science & Technology*, 46, 4275-4282, 10.1021/es203325a, 2012.
- 838 Benduhn, F., Mann, G. W., Pringle, K. J., Topping, D. O., McFiggans, G., and Carslaw, K. S.: Size-resolved
839 simulations of the aerosol inorganic composition with the new hybrid dissolution solver HyDiS-1.0 –
840 Description, evaluation and first global modelling results, *Geosci. Model Dev. Discuss.*, 2016, 1-54,
841 10.5194/gmd-2015-264, 2016.
- 842 Bond, T. C., Streets, D. G., Yarber, K. F., Nelson, S. M., Woo, J.-H., and Klimont, Z.: A technology-based global
843 inventory of black and organic carbon emissions from combustion, *Journal of Geophysical Research:*
844 *Atmospheres*, 109, D14203, 10.1029/2003JD003697, 2004.
- 845 Bouwman, A. F., Lee, D. S., Asman, W. A. H., Dentener, F. J., Van Der Hoek, K. W., and Olivier, J. G. J.: A global
846 high-resolution emission inventory for ammonia, *Global Biogeochemical Cycles*, 11, 561-587,
847 10.1029/97GB02266, 1997.

848 Brasseur, G. P., Gupta, M., Anderson, B. E., Balasubramanian, S., Barrett, S., Duda, D., Fleming, G., Forster, P.
849 M., Fuglestedt, J., Gettelman, A., Halthore, R. N., Jacob, S. D., Jacobson, M. Z., Khodayari, A., Liou, K.-N.,
850 Lund, M. T., Miake-Lye, R. C., Minnis, P., Olsen, S., Penner, J. E., Prinn, R., Schumann, U., Selkirk, H. B.,
851 Sokolov, A., Unger, N., Wolfe, P., Wong, H.-W., Wuebbles, D. W., Yi, B., Yang, P., and Zhou, C.: Impact of
852 Aviation on Climate: FAA's Aviation Climate Change Research Initiative (ACCRI) Phase II, Bulletin of the
853 American Meteorological Society, 10.1175/BAMS-D-13-00089.1, 2015.

854 Breider, T. J., Chipperfield, M. P., Richards, N. A. D., Carslaw, K. S., Mann, G. W., and Spracklen, D. V.: Impact
855 of BrO on dimethylsulfide in the remote marine boundary layer, Geophysical Research Letters, 37, L02807,
856 10.1029/2009GL040868, 2010.

857 Burkhardt, U., and Karcher, B.: Global radiative forcing from contrail cirrus, Nature Clim. Change, 1, 54-58,
858 2011.

859 Burnett, R. T., Pope, C. A., Ezzati, M., Olives, C., Lim, S. S., Mehta, S., Shin, H. H., Singh, G., Hubbell, B., and
860 Brauer, M.: An integrated risk function for estimating the global burden of disease attributable to ambient
861 fine particulate matter exposure, 2014.

862 Chipperfield, M. P.: New version of the TOMCAT/SLIMCAT off-line chemical transport model:
863 Intercomparison of stratospheric tracer experiments, Quarterly Journal of the Royal Meteorological Society,
864 132, 1179-1203, 10.1256/qj.05.51, 2006.

865 Chipperfield, M. P., Dhomse, S. S., Feng, W., McKenzie, R. L., Velders, G. J. M., and Pyle, J. A.: Quantifying the
866 ozone and ultraviolet benefits already achieved by the Montreal Protocol, Nat Commun, 6,
867 10.1038/ncomms8233, 2015.

868 Cofala, J., Amann, M., Klimont, Z., and Schopp, W.: Scenarios of World Anthropogenic Emissions of SO₂, NO_x
869 and CO up to 2030, International Institute for Applied Systems Analysis, Laxenburg, Austria, 2005.

870 Dentener, F., Kinne, S., Bond, T., Boucher, O., Cofala, J., Generoso, S., Ginoux, P., Gong, S., Hoelzemann, J. J.,
871 Ito, A., Marelli, L., Penner, J. E., Putaud, J. P., Textor, C., Schulz, M., van der Werf, G. R., and Wilson, J.:
872 Emissions of primary aerosol and precursor gases in the years 2000 and 1750 prescribed data-sets for
873 AeroCom, Atmos. Chem. Phys., 6, 4321-4344, 10.5194/acp-6-4321-2006, 2006.

874 Dessens, O., Köhler, M. O., Rogers, H. L., Jones, R. L., and Pyle, J. A.: Aviation and climate change, Transport
875 Policy, <http://dx.doi.org/10.1016/j.tranpol.2014.02.014>, 2014.

876 Dockery, D. W., Pope, C. A., Xu, X., Spengler, J. D., Ware, J. H., Fay, M. E., Ferris, B. G., and Speizer, F. E.: An
877 Association between Air Pollution and Mortality in Six U.S. Cities, New England Journal of Medicine, 329,
878 1753-1759, doi:10.1056/NEJM199312093292401, 1993.

879 DuBois, D., and Paynter, G. C.: "Fuel Flow Method2" for Estimating Aircraft Emissions, SAE Technical Paper
880 Series, 01, 2006.

881 Eckhardt, S., Quennehen, B., Olivié, D. J. L., Berntsen, T. K., Cherian, R., Christensen, J. H., Collins, W.,
882 Crepinsek, S., Daskalakis, N., Flanner, M., Herber, A., Heyes, C., Hodnebrog, Ø., Huang, L., Kanakidou, M.,
883 Klimont, Z., Langner, J., Law, K. S., Lund, M. T., Mahmood, R., Massling, A., Myriokefalitakis, S., Nielsen, I. E.,
884 Nøjgaard, J. K., Quaas, J., Quinn, P. K., Raut, J. C., Rumbold, S. T., Schulz, M., Sharma, S., Skeie, R. B., Skov, H.,
885 Uttal, T., von Salzen, K., and Stohl, A.: Current model capabilities for simulating black carbon and sulfate
886 concentrations in the Arctic atmosphere: a multi-model evaluation using a comprehensive measurement
887 data set, Atmos. Chem. Phys., 15, 9413-9433, 10.5194/acp-15-9413-2015, 2015.

888 Edwards, J. M., and Slingo, A.: Studies with a flexible new radiation code. I: Choosing a configuration for a
889 large-scale model, Quarterly Journal of the Royal Meteorological Society, 122, 689-719,
890 10.1002/qj.49712253107, 1996.

891 Eysers, C. J., Addleton, D., Atkinson, K., Broomhead, M. J., Christou, R., Elliff, T., Falk, R., Gee, I., Lee, D. S.,
892 Marizy, C., S Michot, Middel, J., Newton, P., Norman, P., Plohr, M., Raper, D., and Stanciou, N.: AERO2K
893 Global Aviation Emissions Inventories for 2002 and 2025, QINETIQ/04/01113, 2004.

894 Eyring, V., Isaksen, I. S. A., Berntsen, T., Collins, W. J., Corbett, J. J., Endresen, O., Grainger, R. G., Moldanova,
895 J., Schlager, H., and Stevenson, D. S.: Transport impacts on atmosphere and climate: Shipping, Atmospheric
896 Environment, 44, 4735-4771, <http://dx.doi.org/10.1016/j.atmosenv.2009.04.059>, 2010.

897 Fiore, A. M., Naik, V., Spracklen, D. V., Steiner, A., Unger, N., Prather, M., Bergmann, D., Cameron-Smith, P.
898 J., Cionni, I., Collins, W. J., Dalsoren, S., Eyring, V., Folberth, G. A., Ginoux, P., Horowitz, L. W., Josse, B.,
899 Lamarque, J.-F., MacKenzie, I. A., Nagashima, T., O'Connor, F. M., Righi, M., Rumbold, S. T., Shindell, D. T.,
900 Skeie, R. B., Sudo, K., Szopa, S., Takemura, T., and Zeng, G.: Global air quality and climate, Chemical Society
901 Reviews, 41, 6663-6683, 2012.

902 Fountoukis, C., and Nenes, A.: Continued development of a cloud droplet formation parameterization for
903 global climate models, *Journal of Geophysical Research: Atmospheres*, 110, D11212,
904 10.1029/2004JD005591, 2005.

905 Frömming, C., Ponater, M., Dahmann, K., Grewe, V., Lee, D. S., and Sausen, R.: Aviation-induced radiative
906 forcing and surface temperature change in dependency of the emission altitude, *J. Geophys. Res.*, 117,
907 D19104, 10.1029/2012JD018204, 2012.

908 Fuglestad, J., Berntsen, T., Myhre, G., Rypdal, K., and Skeie, R. B.: Climate forcing from the transport
909 sectors, *Proceedings of the National Academy of Sciences*, 105, 454-458, 10.1073/pnas.0702958104, 2008.

910 Gettelman, A., and Chen, C.: The climate impact of aviation aerosols, *Geophysical Research Letters*, 40, 2785-
911 2789, 10.1002/grl.50520, 2013.

912 Guenther, A., Hewitt, C. N., Erickson, D., Fall, R., Geron, C., Graedel, T., Harley, P., Klinger, L., Lerdau, M.,
913 McKay, W. A., Pierce, T., Scholes, B., Steinbrecher, R., Tallamraju, R., Taylor, J., and Zimmerman, P.: A global
914 model of natural volatile organic compound emissions, *Journal of Geophysical Research: Atmospheres*, 100,
915 8873-8892, 10.1029/94JD02950, 1995.

916 Halmer, M. M., Schmincke, H. U., and Graf, H. F.: The annual volcanic gas input into the atmosphere, in
917 particular into the stratosphere: a global data set for the past 100 years, *Journal of Volcanology and
918 Geothermal Research*, 115, 511-528, [http://dx.doi.org/10.1016/S0377-0273\(01\)00318-3](http://dx.doi.org/10.1016/S0377-0273(01)00318-3), 2002.

919 Hand, J. L., Schichtel, B. A., Malm, W. C., and Pitchford, M. L.: Particulate sulfate ion concentration and SO₂
920 emission trends in the United States from the early 1990s through 2010, *Atmos. Chem. Phys.*, 12, 10353-
921 10365, 10.5194/acp-12-10353-2012, 2012.

922 Heald, C. L., Coe, H., Jimenez, J. L., Weber, R. J., Bahreini, R., Middlebrook, A. M., Russell, L. M., Jolleys, M.,
923 Fu, T. M., Allan, J. D., Bower, K. N., Capes, G., Crosier, J., Morgan, W. T., Robinson, N. H., Williams, P. I.,
924 Cubison, M. J., DeCarlo, P. F., and Dunlea, E. J.: Exploring the vertical profile of atmospheric organic aerosol:
925 comparing 17 aircraft field campaigns with a global model, *Atmos. Chem. Phys.*, 11, 12673-12696,
926 10.5194/acp-11-12673-2011, 2011.

927 Hileman, J. I., and Stratton, R. W.: Alternative jet fuel feasibility, *Transport Policy*,
928 <http://dx.doi.org/10.1016/j.tranpol.2014.02.018>, 2014.

929 Holmes, C. D., Tang, Q., and Prather, M. J.: Uncertainties in climate assessment for the case of aviation NO_x,
930 *Proceedings of the National Academy of Sciences*, 108, 10997-11002, 10.1073/pnas.1101458108, 2011.

931 Hoor, P., Borken-Kleefeld, J., Caro, D., Dessens, O., Endresen, O., Gauss, M., Grewe, V., Hauglustaine, D.,
932 Isaksen, I. S. A., Jöckel, P., Lelieveld, J., Myhre, G., Meijer, E., Olivier, D., Prather, M., Schnadt Poberaj, C.,
933 Shine, K. P., Staehelin, J., Tang, Q., van Aardenne, J., van Velthoven, P., and Sausen, R.: The impact of traffic
934 emissions on atmospheric ozone and OH: results from QUANTIFY, *Atmos. Chem. Phys.*, 9, 3113-3136,
935 10.5194/acp-9-3113-2009, 2009.

936 Hopke, P. K.: *Receptor modeling in environmental chemistry*, v. 76, Wiley, 1985.

937 ICAO: *Annual Report of the Council 2012*, International Civil Aviation Organisation (ICAO), 2013.

938 Jacobson, M. Z., Wilkerson, J. T., Naiman, A. D., and Lele, S. K.: The effects of aircraft on climate and
939 pollution. Part II: 20-year impacts of exhaust from all commercial aircraft worldwide treated individually at
940 the subgrid scale, *Faraday Discussions*, 165, 369-382, 10.1039/C3FD00034F, 2013.

941 Kaiser, J. W., Heil, A., Andreae, M. O., Benedetti, A., Chubarova, N., Jones, L., Morcrette, J. J., Razinger, M.,
942 Schultz, M. G., Suttie, M., and van der Werf, G. R.: Biomass burning emissions estimated with a global fire
943 assimilation system based on observed fire radiative power, *Biogeosciences*, 9, 527-554, 10.5194/bg-9-527-
944 2012, 2012.

945 Kettle, A. J., and Andreae, M. O.: Flux of dimethylsulfide from the oceans: A comparison of updated data sets
946 and flux models, *Journal of Geophysical Research: Atmospheres*, 105, 26793-26808, 10.1029/2000JD900252,
947 2000.

948 Khodayari, A., Olsen, S. C., and Wuebbles, D. J.: Evaluation of aviation NO_x-induced radiative forcings for
949 2005 and 2050, *Atmospheric Environment*, 91, 95-103, <http://dx.doi.org/10.1016/j.atmosenv.2014.03.044>,
950 2014.

951 Knighton, W. B., Rogers, T. M., Anderson, B. E., Herndon, S. C., Yelvington, P. E., and Miake-Lye, R. C.:
952 Quantification of Aircraft Engine Hydrocarbon Emissions Using Proton Transfer Reaction Mass Spectrometry,
953 *Journal of Propulsion and Power*, 23, 949-958, 2007.

954 Knippertz, P., Evans, M. J., Field, P. R., Fink, A. H., Lioussé, C., and Marsham, J. H.: The possible role of local
955 air pollution in climate change in West Africa, *Nature Clim. Change*, 5, 815-822, 10.1038/nclimate2727, 2015.

956 Köhler, M. O., Rädcl, G., Dessens, O., Shine, K. P., Rogers, H. L., Wild, O., and Pyle, J. A.: Impact of
957 perturbations to nitrogen oxide emissions from global aviation, *Journal of Geophysical Research:*
958 *Atmospheres*, 113, D11305, 10.1029/2007JD009140, 2008.

959 Köhler, M. O., Rädcl, G., Shine, K. P., Rogers, H. L., and Pyle, J. A.: Latitudinal variation of the effect of
960 aviation NO_x emissions on atmospheric ozone and methane and related climate metrics, *Atmospheric*
961 *Environment*, 64, 1-9, 10.1016/j.atmosenv.2012.09.013, 2013.

962 Konovalov, I. B., Beekmann, M., Burrows, J. P., and Richter, A.: Satellite measurement based estimates of
963 decadal changes in European nitrogen oxides emissions, *Atmos. Chem. Phys.*, 8, 2623-2641, 10.5194/acp-8-
964 2623-2008, 2008.

965 Lamarque, J. F., Hess, P., Emmons, L., Buja, L., Washington, W., and Granier, C.: Tropospheric ozone
966 evolution between 1890 and 1990, *Journal of Geophysical Research: Atmospheres*, 110, n/a-n/a,
967 10.1029/2004JD005537, 2005.

968 Lamarque, J. F., Bond, T. C., Eyring, V., Granier, C., Heil, A., Klimont, Z., Lee, D., Liousse, C., Mieville, A., Owen,
969 B., Schultz, M. G., Shindell, D., Smith, S. J., Stehfest, E., Van Aardenne, J., Cooper, O. R., Kainuma, M.,
970 Mahowald, N., McConnell, J. R., Naik, V., Riahi, K., and van Vuuren, D. P.: Historical (1850–2000) gridded
971 anthropogenic and biomass burning emissions of reactive gases and aerosols: methodology and application,
972 *Atmos. Chem. Phys.*, 10, 7017-7039, 10.5194/acp-10-7017-2010, 2010.

973 Lee, D. S., Fahey, D. W., Forster, P. M., Newton, P. J., Wit, R. C. N., Lim, L. L., Owen, B., and Sausen, R.:
974 Aviation and global climate change in the 21st century, *Atmospheric Environment*, 43, 3520-3537,
975 10.1016/j.atmosenv.2009.04.024, 2009.

976 Lee, D. S., Pitari, G., Grewe, V., Gierens, K., Penner, J. E., Petzold, A., Prather, M. J., Schumann, U., Bais, A.,
977 Berntsen, T., Iachetti, D., Lim, L. L., and Sausen, R.: Transport impacts on atmosphere and climate: Aviation,
978 *Atmospheric Environment*, 44, 4678-4734, 10.1016/j.atmosenv.2009.06.005, 2010.

979 Lim, S. S., Vos, T., Flaxman, A. D., Danaei, G., Shibuya, K., Adair-Rohani, H., AlMazroa, M. A., Amann, M.,
980 Anderson, H. R., Andrews, K. G., Aryee, M., Atkinson, C., Bacchus, L. J., Bahalim, A. N., Balakrishnan, K.,
981 Balmes, J., Barker-Collo, S., Baxter, A., Bell, M. L., Blore, J. D., Blyth, F., Bonner, C., Borges, G., Bourne, R.,
982 Boussinesq, M., Brauer, M., Brooks, P., Bruce, N. G., Brunekreef, B., Bryan-Hancock, C., Bucello, C.,
983 Buchbinder, R., Bull, F., Burnett, R. T., Byers, T. E., Calabria, B., Carapetis, J., Carnahan, E., Chafe, Z., Charlson,
984 F., Chen, H., Chen, J. S., Cheng, A. T.-A., Child, J. C., Cohen, A., Colson, K. E., Cowie, B. C., Darby, S., Darling, S.,
985 Davis, A., Degenhardt, L., Dentener, F., Des Jarlais, D. C., Devries, K., Dherani, M., Ding, E. L., Dorsey, E. R.,
986 Driscoll, T., Edmond, K., Ali, S. E., Engell, R. E., Erwin, P. J., Fahimi, S., Falder, G., Farzadfar, F., Ferrari, A.,
987 Finucane, M. M., Flaxman, S., Fowkes, F. G. R., Freedman, G., Freeman, M. K., Gakidou, E., Ghosh, S.,
988 Giovannucci, E., Gmel, G., Graham, K., Grainger, R., Grant, B., Gunnell, D., Gutierrez, H. R., Hall, W., Hoek, H.
989 W., Hogan, A., Hosgood Iii, H. D., Hoy, D., Hu, H., Hubbell, B. J., Hutchings, S. J., Ibeanusi, S. E., Jacklyn, G. L.,
990 Jasrasaria, R., Jonas, J. B., Kan, H., Kanis, J. A., Kassebaum, N., Kawakami, N., Khang, Y.-H., Khatibzadeh, S.,
991 Khoo, J.-P., Kok, C., Laden, F., Lalloo, R., Lan, Q., Lathlean, T., Leasher, J. L., Leigh, J., Li, Y., Lin, J. K., Lipshultz,
992 S. E., London, S., Lozano, R., Lu, Y., Mak, J., Malekzadeh, R., Mallinger, L., Marcenes, W., March, L., Marks, R.,
993 Martin, R., McGale, P., McGrath, J., Mehta, S., Memish, Z. A., Mensah, G. A., Merriman, T. R., Micha, R.,
994 Michaud, C., Mishra, V., Hanafiah, K. M., Mokdad, A. A., Morawska, L., Mozaffarian, D., Murphy, T., Naghavi,
995 M., Neal, B., Nelson, P. K., Nolla, J. M., Norman, R., Olives, C., Omer, S. B., Orchard, J., Osborne, R., Ostro, B.,
996 Page, A., Pandey, K. D., Parry, C. D. H., Passmore, E., Patra, J., Pearce, N., Pelizzari, P. M., Petzold, M., Phillips,
997 M. R., Pope, D., Pope III, C. A., Powles, J., Rao, M., Razavi, H., Rehfuss, E. A., Rehm, J. T., Ritz, B., Rivara, F. P.,
998 Roberts, T., Robinson, C., Rodriguez-Portales, J. A., Romieu, I., Room, R., Rosenfeld, L. C., Roy, A., Rushton, L.,
999 Salomon, J. A., Sampson, U., Sanchez-Riera, L., Sanman, E., Sapkota, A., Seedat, S., Shi, P., Shield, K.,
1000 Shivakoti, R., Singh, G. M., Sleet, D. A., Smith, E., Smith, K. R., Stapelberg, N. J. C., Steenland, K., Stöckl, H.,
1001 Stovner, L. J., Straif, K., Straney, L., Thurston, G. D., Tran, J. H., Van Dingenen, R., van Donkelaar, A., Veerman,
1002 J. L., Vijayakumar, L., Weintraub, R., Weissman, M. M., White, R. A., Whiteford, H., Wiersma, S. T., Wilkinson,
1003 J. D., Williams, H. C., Williams, W., Wilson, N., Woolf, A. D., Yip, P., Zielinski, J. M., Lopez, A. D., Murray, C. J.
1004 L., and Ezzati, M.: A comparative risk assessment of burden of disease and injury attributable to 67 risk
1005 factors and risk factor clusters in 21 regions, 1990–2010: a systematic analysis for the Global Burden of
1006 Disease Study 2010, *The Lancet*, 380, 2224-2260, [http://dx.doi.org/10.1016/S0140-6736\(12\)61766-8](http://dx.doi.org/10.1016/S0140-6736(12)61766-8), 2012.

1007 Mann, G. W., Carslaw, K. S., Spracklen, D. V., Ridley, D. A., Manktelow, P. T., Chipperfield, M. P., Pickering, S.
1008 J., and Johnson, C. E.: Description and evaluation of GLOMAP-mode: a modal global aerosol microphysics

1009 model for the UKCA composition-climate model, *Geosci. Model Dev.*, 3, 519-551, 10.5194/gmd-3-519-2010,
1010 2010.

1011 Ministry of Defence: Defence Standard 91-91. Turbine Fuel, Kerosine Type, Jet A-1. NATO Code: F-35. Joint
1012 Service Designation: AVTUR, Glasgow, United Kingdom, 2011.

1013 Morita, H., Yang, S., Unger, N., and Kinney, P. L.: Global Health Impacts of Future Aviation Emissions Under
1014 Alternative Control Scenarios, *Environmental Science & Technology*, 48, 14659-14667, 10.1021/es5055379,
1015 2014.

1016 Myhre, G., Shine, K. P., Rädel, G., Gauss, M., Isaksen, I. S. A., Tang, Q., Prather, M. J., Williams, J. E., van
1017 Velthoven, P., Dessens, O., Koffi, B., Szopa, S., Hoor, P., Grewe, V., Borken-Kleefeld, J., Berntsen, T. K., and
1018 Fuglestvedt, J. S.: Radiative forcing due to changes in ozone and methane caused by the transport sector,
1019 *Atmospheric Environment*, 45, 387-394, 10.1016/j.atmosenv.2010.10.001, 2011.

1020 Nenes, A., and Seinfeld, J. H.: Parameterization of cloud droplet formation in global climate models, *Journal*
1021 *of Geophysical Research: Atmospheres*, 108, 4415, 10.1029/2002JD002911, 2003.

1022 Nightingale, P. D., Malin, G., Law, C. S., Watson, A. J., Liss, P. S., Liddicoat, M. I., Boutin, J., and Upstill-
1023 Goddard, R. C.: In situ evaluation of air-sea gas exchange parameterizations using novel conservative and
1024 volatile tracers, *Global Biogeochemical Cycles*, 14, 373-387, 10.1029/1999GB900091, 2000.

1025 Olsen, S. C., Wuebbles, D. J., and Owen, B.: Comparison of global 3-D aviation emissions datasets, *Atmos.*
1026 *Chem. Phys.*, 13, 429-441, 10.5194/acp-13-429-2013, 2013.

1027 Ostro, B. D.: Outdoor air pollution: Assessing the environmental burden of disease at national and local
1028 levels, 2004.

1029 Pope, C. A., Burnett, R. T., Thun, M. J., Calle, E. E., Krewski, D., Ito, K., and Thurston, G. D.: Lung Cancer,
1030 Cardiopulmonary Mortality, and Long-term Exposure to Fine Particulate Air Pollution, *JAMA*, 287, 1132-1141,
1031 10.1001/jama.287.9.1132, 2002.

1032 Pope, C. A., and Dockery, D. W.: Health effects of fine particulate air pollution: lines that connect, *Journal of*
1033 *the Air & Waste Management Association*, 56, 709-742, 2006.

1034 EU FP6 Integrated Project QUANTIFY. Quantifying the Climate Impact of Global and European Transport
1035 Systems: QUANTIFY emission inventories and scenarios: <http://www.pa.op.dlr.de/quantify/>, access:
1036 15/07/2011, 2005-2012.

1037 Rap, A., Forster, P. M., Jones, A., Boucher, O., Haywood, J. M., Bellouin, N., and De Leon, R. R.:
1038 Parameterization of contrails in the UK Met Office Climate Model, *J. Geophys. Res.*, 115, D10205,
1039 10.1029/2009jd012443, 2010.

1040 Rap, A., Scott, C. E., Spracklen, D. V., Bellouin, N., Forster, P. M., Carslaw, K. S., Schmidt, A., and Mann, G.:
1041 Natural aerosol direct and indirect radiative effects, *Geophysical Research Letters*, 40, 3297-3301,
1042 10.1002/grl.50441, 2013.

1043 Rap, A., Richards, N. A. D., Forster, P. M., Monks, S. A., Arnold, S. R., and Chipperfield, M. P.: Satellite
1044 constraint on the tropospheric ozone radiative effect, *Geophysical Research Letters*, 42, 2015GL064037,
1045 10.1002/2015GL064037, 2015.

1046 Ratliff, G., Sequeira, C., Waitz, I., Ohsfeldt, M., Thrasher, T., Graham, M., and Thompson, T.: Aircraft Impacts
1047 on Local and Regional Air Quality in the United States, Massachusetts Institute of Technology PARTNER
1048 report (Report No. PARTNER-COE-2009-002), 2009.

1049 Richards, N. A. D., Arnold, S. R., Chipperfield, M. P., Miles, G., Rap, A., Siddans, R., Monks, S. A., and
1050 Hollaway, M. J.: The Mediterranean summertime ozone maximum: global emission sensitivities and radiative
1051 impacts, *Atmos. Chem. Phys.*, 13, 2331-2345, 10.5194/acp-13-2331-2013, 2013.

1052 Righi, M., Hendricks, J., and Sausen, R.: The global impact of the transport sectors on atmospheric aerosol:
1053 simulations for year 2000 emissions, *Atmos. Chem. Phys.*, 13, 9939-9970, 10.5194/acp-13-9939-2013, 2013.

1054 Rossow, W. B., and Schiffer, R. A.: Advances in Understanding Clouds from ISCCP, *Bulletin of the American*
1055 *Meteorological Society*, 80, 2261-2287, 10.1175/1520-0477(1999)080<2261:AIUCFI>2.0.CO;2, 1999.

1056 Sausen, R., Isaksen, I., Grewe, V., Hauglustaine, D., Lee, D. S., Myhre, G., Köhler, M. O., Pitari, G., Schumann,
1057 U., Stordal, F., and Zerefos, C.: Aviation radiative forcing in 2000: An update on IPCC (1999), *Meteorologische*
1058 *Zeitschrift*, 14, 555-561, 2005.

1059 Schmidt, A., Carslaw, K. S., Mann, G. W., Rap, A., Pringle, K. J., Spracklen, D. V., Wilson, M., and Forster, P.
1060 M.: Importance of tropospheric volcanic aerosol for indirect radiative forcing of climate, *Atmos. Chem. Phys.*,
1061 12, 7321-7339, 10.5194/acp-12-7321-2012, 2012.

1062 Shindell, D. T., Chin, M., Dentener, F., Doherty, R. M., Faluvegi, G., Fiore, A. M., Hess, P., Koch, D. M.,
1063 MacKenzie, I. A., Sanderson, M. G., Schultz, M. G., Schulz, M., Stevenson, D. S., Teich, H., Textor, C., Wild, O.,
1064 Bergmann, D. J., Bey, I., Bian, H., Cuvelier, C., Duncan, B. N., Folberth, G., Horowitz, L. W., Jonson, J.,
1065 Kaminski, J. W., Marmer, E., Park, R., Pringle, K. J., Schroeder, S., Szopa, S., Takemura, T., Zeng, G., Keating, T.
1066 J., and Zuber, A.: A multi-model assessment of pollution transport to the Arctic, *Atmos. Chem. Phys.*, **8**, 5353-
1067 5372, 10.5194/acp-8-5353-2008, 2008.

1068 Skowron, A., Lee, D. S., and De León, R. R.: The assessment of the impact of aviation NO_x on ozone and other
1069 radiative forcing responses – The importance of representing cruise altitudes accurately, *Atmospheric*
1070 *Environment*, **74**, 159-168, <http://dx.doi.org/10.1016/j.atmosenv.2013.03.034>, 2013.

1071 Spicer, C. W., Holdren, M. W., Riggin, R. M., and Lyon, T. F.: Chemical composition and photochemical
1072 reactivity of exhaust from aircraft turbine engines, *Ann. Geophys.*, **12**, 944-955, 10.1007/s00585-994-0944-0,
1073 1994.

1074 Spracklen, D. V., Pringle, K. J., Carslaw, K. S., Chipperfield, M. P., and Mann, G. W.: A global off-line model of
1075 size-resolved aerosol microphysics: I. Model development and prediction of aerosol properties, *Atmospheric*
1076 *Chemistry and Physics*, **5**, 2227-2252, 2005.

1077 Spracklen, D. V., Carslaw, K. S., Merikanto, J., Mann, G. W., Reddington, C. L., Pickering, S., Ogren, J. A.,
1078 Andrews, E., Baltensperger, U., Weingartner, E., Boy, M., Kulmala, M., Laakso, L., Lihavainen, H., Kivekäs, N.,
1079 Komppula, M., Mihalopoulos, N., Kouvarakis, G., Jennings, S. G., O'Dowd, C., Birmili, W., Wiedensohler, A.,
1080 Weller, R., Gras, J., Laj, P., Sellegri, K., Bonn, B., Krejci, R., Laaksonen, A., Hamed, A., Minikin, A., Harrison, R.
1081 M., Talbot, R., and Sun, J.: Explaining global surface aerosol number concentrations in terms of primary
1082 emissions and particle formation, *Atmos. Chem. Phys.*, **10**, 4775-4793, 10.5194/acp-10-4775-2010, 2010.

1083 Spracklen, D. V., Carslaw, K. S., Pöschl, U., Rap, A., and Forster, P. M.: Global cloud condensation nuclei
1084 influenced by carbonaceous combustion aerosol, *Atmos. Chem. Phys.*, **11**, 9067-9087, 10.5194/acp-11-9067-
1085 2011, 2011a.

1086 Spracklen, D. V., Jimenez, J. L., Carslaw, K. S., Worsnop, D. R., Evans, M. J., Mann, G. W., Zhang, Q.,
1087 Canagaratna, M. R., Allan, J., Coe, H., McFiggans, G., Rap, A., and Forster, P.: Aerosol mass spectrometer
1088 constraint on the global secondary organic aerosol budget, *Atmos. Chem. Phys.*, **11**, 12109-12136,
1089 10.5194/acp-11-12109-2011, 2011b.

1090 Stevenson, D. S., and Derwent, R. G.: Does the location of aircraft nitrogen oxide emissions affect their
1091 climate impact?, *Geophysical Research Letters*, **36**, L17810, 10.1029/2009GL039422, 2009.

1092 Stevenson, D. S., Young, P. J., Naik, V., Lamarque, J. F., Shindell, D. T., Voulgarakis, A., Skeie, R. B., Dalsoren,
1093 S. B., Myhre, G., Berntsen, T. K., Folberth, G. A., Rumbold, S. T., Collins, W. J., MacKenzie, I. A., Doherty, R.
1094 M., Zeng, G., van Noije, T. P. C., Strunk, A., Bergmann, D., Cameron-Smith, P., Plummer, D. A., Strode, S. A.,
1095 Horowitz, L., Lee, Y. H., Szopa, S., Sudo, K., Nagashima, T., Josse, B., Cionni, I., Righi, M., Eyring, V., Conley, A.,
1096 Bowman, K. W., Wild, O., and Archibald, A.: Tropospheric ozone changes, radiative forcing and attribution to
1097 emissions in the Atmospheric Chemistry and Climate Model Intercomparison Project (ACCMIP), *Atmos.*
1098 *Chem. Phys.*, **13**, 3063-3085, 10.5194/acp-13-3063-2013, 2013.

1099 Thompson, A. M., Tao, W.-K., Pickering, K. E., Scala, J. R., and Simpson, J.: Tropical Deep Convection and
1100 Ozone Formation, *Bulletin of the American Meteorological Society*, **78**, 1043-1054, 10.1175/1520-
1101 0477(1997)078<1043:TDCAOF>2.0.CO;2, 1997.

1102 Tilmes, S., Lamarque, J. F., Emmons, L. K., Conley, A., Schultz, M. G., Saunio, M., Thouret, V., Thompson, A.
1103 M., Oltmans, S. J., Johnson, B., and Tarasick, D.: Technical Note: Ozone sonde climatology between 1995 and
1104 2011: description, evaluation and applications, *Atmos. Chem. Phys.*, **12**, 7475-7497, 10.5194/acp-12-7475-
1105 2012, 2012.

1106 Uherek, E., Halenka, T., Borcken-Kleefeld, J., Balkanski, Y., Berntsen, T., Borrego, C., Gauss, M., Hoor, P., Juda-
1107 Rezler, K., Lelieveld, J., Melas, D., Rypdal, K., and Schmid, S.: Transport impacts on atmosphere and climate:
1108 Land transport, *Atmospheric Environment*, **44**, 4772-4816,
1109 <http://dx.doi.org/10.1016/j.atmosenv.2010.01.002>, 2010.

1110 Unger, N., Shindell, D. T., Koch, D. M., and Streets, D. G.: Cross influences of ozone and sulfate precursor
1111 emissions changes on air quality and climate, *Proceedings of the National Academy of Sciences of the United*
1112 *States of America*, **103**, 4377-4380, 10.1073/pnas.0508769103, 2006.

1113 Unger, N.: Global climate impact of civil aviation for standard and desulfurized jet fuel, *Geophys. Res. Lett.*,
1114 **38**, L20803, 10.1029/2011gl049289, 2011.

1115 Unger, N., Zhao, Y., and Dang, H.: Mid-21st century chemical forcing of climate by the civil aviation sector,
1116 Geophysical Research Letters, 40, 641-645, 10.1002/grl.50161, 2013.

1117 Van Der Werf, G. R., Randerson, J. T., Collatz, G. J., and Giglio, L.: Carbon emissions from fires in tropical and
1118 subtropical ecosystems, Global Change Biology, 9, 547-562, 10.1046/j.1365-2486.2003.00604.x, 2003.

1119 van der Werf, G. R., Randerson, J. T., Giglio, L., Collatz, G. J., Mu, M., Kasibhatla, P. S., Morton, D. C., DeFries,
1120 R. S., Jin, Y., and van Leeuwen, T. T.: Global fire emissions and the contribution of deforestation, savanna,
1121 forest, agricultural, and peat fires (1997–2009), Atmos. Chem. Phys., 10, 11707-11735, 10.5194/acp-10-
1122 11707-2010, 2010.

1123 Vestreng, V., Myhre, G., Fagerli, H., Reis, S., and Tarrasón, L.: Twenty-five years of continuous sulphur dioxide
1124 emission reduction in Europe, Atmos. Chem. Phys., 7, 3663-3681, 10.5194/acp-7-3663-2007, 2007.

1125 Wayson, R. L., Fleming, G. G., and Iovinelli, R.: Methodology to Estimate Particulate Matter Emissions from
1126 Certified Commercial Aircraft Engines, Journal of the Air & Waste Management Association, 59, 91-100,
1127 10.3155/1047-3289.59.1.91, 2009.

1128 Whitburn, S., Van Damme, M., Kaiser, J. W., van der Werf, G. R., Turquety, S., Hurtmans, D., Clarisse, L.,
1129 Clerbaux, C., and Coheur, P. F.: Ammonia emissions in tropical biomass burning regions: Comparison
1130 between satellite-derived emissions and bottom-up fire inventories, Atmospheric Environment,
1131 <http://dx.doi.org/10.1016/j.atmosenv.2015.03.015>, 2015.

1132 Wiedinmyer, C., Akagi, S. K., Yokelson, R. J., Emmons, L. K., Al-Saadi, J. A., Orlando, J. J., and Soja, A. J.: The
1133 Fire INventory from NCAR (FINN): a high resolution global model to estimate the emissions from open
1134 burning, Geosci. Model Dev., 4, 625-641, 10.5194/gmd-4-625-2011, 2011.

1135 Wilkerson, J. T., Jacobson, M. Z., Malwitz, A., Balasubramanian, S., Wayson, R., Fleming, G., Naiman, A. D.,
1136 and Lele, S. K.: Analysis of emission data from global commercial aviation: 2004 and 2006, Atmos. Chem.
1137 Phys., 10, 6391-6408, 10.5194/acp-10-6391-2010, 2010.

1138 Woody, M., Haeng Baek, B., Adelman, Z., Omary, M., Fat Lam, Y., Jason West, J., and Arunachalam, S.: An
1139 assessment of Aviation's contribution to current and future fine particulate matter in the United States,
1140 Atmospheric Environment, 45, 3424-3433, 10.1016/j.atmosenv.2011.03.041, 2011.

1141 World Health Organisation: Health Aspects of Air Pollution with Particulate Matter, Ozone and Nitrogen
1142 Dioxide, Bonn, Germany, 2003.

1143 World Health Organisation: Air Quality Guidelines a Global Update 2005: Particulate matter, ozone, nitrogen
1144 dioxide and sulphur dioxide, Germany, 2005.

1145 Yim, N.-H., Kim, S.-H., Kim, H.-W., and Kwahk, K.-Y.: Knowledge based decision making on higher level
1146 strategic concerns: system dynamics approach, Expert Systems with Applications, 27, 143-158, DOI:
1147 10.1016/j.eswa.2003.12.019, 2004.

1148 Yim, S. H. L., Lee, G. L., Lee, I. H., Allroggen, F., Ashok, A., Caiazza, F., Eastham, S. D., Malina, R., and Barrett,
1149 S. R. H.: Global, regional and local health impacts of civil aviation emissions, Environmental Research Letters,
1150 10, 034001, 2015.

1151 Young, P. J., Archibald, A. T., Bowman, K. W., Lamarque, J. F., Naik, V., Stevenson, D. S., Tilmes, S.,
1152 Voulgarakis, A., Wild, O., Bergmann, D., Cameron-Smith, P., Cionni, I., Collins, W. J., Dalsøren, S. B., Doherty,
1153 R. M., Eyring, V., Faluvegi, G., Horowitz, L. W., Josse, B., Lee, Y. H., MacKenzie, I. A., Nagashima, T., Plummer,
1154 D. A., Righi, M., Rumbold, S. T., Skeie, R. B., Shindell, D. T., Strode, S. A., Sudo, K., Szopa, S., and Zeng, G.: Pre-
1155 industrial to end 21st century projections of tropospheric ozone from the Atmospheric Chemistry and
1156 Climate Model Intercomparison Project (ACCMIP), Atmos. Chem. Phys., 13, 2063-2090, 10.5194/acp-13-
1157 2063-2013, 2013.

1158

1159

1160

1161

1162

1163

1164

1165

1166

1167

1168

1169
1170
1171
1172
1173
1174
1175
1176
1177
1178
1179
1180
1181
1182
1183
1184
1185
1186
1187
1188
1189
1190
1191